*Transport in Porous Media* **20:** 135–168, 1995.



# Generalized Relative Permeability Coefficients during Steady-State Two-Phase Flow in Porous Media, and Correlation with the Flow Mechanisms

D. G. AVRAAM and A. C. PAYATAKES
*Department of Chemical Engineering, University of Patras, and Institute of Chemical Engineering and High Temperature Chemical Processes, PO Box 1414, GR 26500 Patras, Greece*

(Received: 7 June 1994; in final form: 14 November 1994)

**Abstract.** A parametric experimental investigation of the coupling effects during steady-state two-phase flow in porous media was carried out using a large model pore network of the chamber-and-throat type, etched in glass. The wetting phase saturation, $S_1$, the capillary number, $Ca$, and the viscosity ratio, $\kappa$, were changed systematically, whereas the wettability (contact angle $\theta_e$), the coalescence factor $Co$, and the geometrical and topological parameters were kept constant. The fluid flow rate and the pressure drop were measured independently for each fluid. During each experiment, the pore-scale flow mechanisms were observed and videorecorded, and the mean water saturation was determined with image analysis. Conventional relative permeability, as well as generalized relative permeability coefficients (with the viscous coupling terms taken explicitly into account) were determined with a new method that is based on a B-spline functional representation combined with standard constrained optimization techniques. A simple relationship between the conventional relative permeabilities and the generalized relative permeability coefficients is established based on several experimental sets. The viscous coupling (off-diagonal) coefficients are found to be comparable in magnitude to the direct (diagonal) coefficients over board ranges of the flow parameter values. The off-diagonal coefficients ($k_{rij}/\mu_j$) are found to be unequal, and this is explained by the fact that, in the class of flows under consideration, microscopic reversibility does not hold and thus the Onsager–Casimir reciprocal relation does not apply. The *coupling indices* are introduced here; they are defined so that the magnitude of each coupling index is the measure of the contribution of the coupling effects to the flow rate of the corresponding fluid. A correlation of the coupling indices with the underlying flow mechanisms and the pertinent flow parameters is established.

**Key words:** two-phase flow, relative permeabilities, ganglion dynamics, viscous coupling, coupling indices.

## 1. Nomenclature

$Bo$ = bond number.
$Ca$ = capillary number = $\mu_1 q_1/\gamma_{12} wl$.
$Co$ = coalescence factor (effective probability of coalescence, given a collision between two ganglia in the porous medium).
$C_k^i$ = parameters used in the functional representation of $k_{ri}$ in terms of cubic B-splines, (Equation (10a)).
$C_k^{ij}$ = parameters used in the functional representation of $k_{rij}$ in terms of cubic B-splines, (Equation (10b)).

$e_{\mu\alpha}$ = residual for the $\mu$th experiment and the $\alpha$th equation of the model, (Equation (6)).
$\mathbf{e}$ = vector of residuals, $e_{\mu\alpha}$.
$k$ = absolute permeability.
$k_{ri}$ = (conventional) relative permeability to fluid $i$.
$k_{ri}^{\circ}$ = value of $k_{ri}$ free from end and boundary effects.
$k_{rij}$ = generalized relative permeability coefficients.
$k_{rij}^{\circ}$ = value of $k_{rij}$ free from end and boundary effects.
$L$ = distance along which $\Delta P_1$ and $\Delta P_2$ are measured.
$l$ = node-to-node distance of the pore network.
$l_\alpha$ = number of unknown parameters in the $\alpha$th equation of the model.
$N$ = number of cubic B-splines used to represent $k_{ri}$ or $k_{rij}$, ((Equation (10a,b)).
$n$ = number of experimental data.
$q_i$ = flowrate of fluid $i$.
$S_i$ = saturation of fluid $i$.
$v_i$ = superficial velocity of fluid $i$.
$\mathbf{V}$ = covariance matrix of the true errors $\varepsilon_{\mu\alpha}$, for all experiments ($\mu$) and equations ($\alpha$) of the model.
$\mathbf{W}$ = weighing matrix, (Equation (7)).
$w$ = width of the network.
$\mathbf{x}$ = vector of the independent variables, (Equation (5)).
$\mathbf{y}$ = vector of the dependent variables.

*Greek Letters*

$\gamma_{12}$ = interfacial tension.
$\varepsilon_{\mu\alpha}$ = true error for the $\mu$th experiment and the $\alpha$th equation.
$\Delta P_i$ = pressure drop (negative) in fluid $i$, along a distance $L$.
$\theta_e$ = equilibrium contact angle.
$\theta$ = vector of unknown parameters, (Equations (5) and (7)).
$\theta^*$ = value of $\theta$ that minimizes the objective function $\Phi$, (Equation (7)).
$\hat{\theta}$ = true (but unknown) value of $\theta$.
$\kappa$ = $\mu_2/\mu_1$ = viscosity ratio.
$\mu_i$ = viscosity of fluid i.
$\sigma_{\mu\alpha}^2$ = variance of the error in the $\mu$th experiment and in the $\alpha$th equation.
$\Phi$ = objective function, (Equation (7)).
$\Phi^{(1)}, \Phi^{(2)}$ = objective function for Model 1 and Model 2, respectively, (Equations (9a)–(b)).
$\chi_i$ = coupling index for fluid $i$.
$\chi_i^{\circ}$ = value of $\chi_i$ free from end and boundary effects.

*Subscripts*

1 water.
2 oil.

## 2. Introduction

Immiscible two-phase flow in porous media is encountered in many processes of great interest, such as oil recovery, agricultural irrigation, pollution of ground

water aquifers by liquid wastes, etc. Such flows can have various modes: imbibition, drainage, steady-state, co-current, counter-current, etc. Here we are concerned with steady-state co-current flow of two immiscible fluids, water (short for wetting fluid; fluid 1), and oil (short for non-wetting fluid; fluid 2).

Recently, it has become clear that the interactions between the two fluids (viscous coupling effects) can be significant for a wide range of two-phase flow cases. However, there are still several important problems to be solved. Key among these are: (a) to develop a reliable and convenient method to obtain the values of all four generalized relative permeability coefficients from steady-state flow rate vs. pressure drop data, and (b) to correlate these coefficients with the pore-level flow mechanisms and, eventually, to understand the coupling effects in quantitative terms. In the present work, a multivariable nonlinear parameter estimation method is used to determine the generalized relative permeability coefficients, with the viscous coupling coefficients taken explicitly into account, during steady-state co-current two-phase flow experiments. In addition, the corresponding conventional relative permeabilities are also evaluated, from the same experimental data. The generalized coefficients are compared with the corresponding conventional relative permeabilities, and all coefficients are correlated with the flow parameters and the underlying flow mechanisms at the pore level, and the flow regimes at the macroscopic scale, in order to quantify the relative importance of the viscous coupling coefficients. A strikingly simple relationship between the generalized relative permeability coefficients and the conventional relative permeabilities, Equation (16), is deduced from theoretical considerations and several sets of experimental results. This relationship helps to explain the reason for which viscous coupling effects are so elusive, despite the fact that they usually are of the first magnitude: they exist embedded in the conventional relative permeabilities and can be extracted only through specially designed means.

Experimental studies of two-phase flow mechanisms are conveniently done in transparent model pore networks etched in glass (Wardlaw, 1982; Chatzis *et al.*, 1983; Lenormand *et al.*, 1983; Chen, 1986; Vizika and Payatakes, 1989; Ioannidis *et al.*, 1991). The experimental results used here have been taken from an experimental study of steady-state co-current two-phase flow in a large planar model pore network of the chamber-and-throat type, etched in glass (Avraam and Payatakes, 1995). In that study, the conventional relative permeabilities to both phases were measured directly using Darcy's law, and then correlated with the corresponding flow regimes. Furthermore, a comparative study of the flow phenomena in both planar and non-planar models of the same type has shown that the flow phenomena remain qualitatively the same, irrespective of the 2-D or 3-D topology (Avraam *et al.*, 1994). This provides justification for using large planar model pore networks. Evaluation of the generalized relative permeability coefficients was not attempted in either of the two aforementioned works for lack of a well established method. The difficulty encountered in such cases is that the four generalized relative permeability coefficients appear in two equations which relate two flow rates ($q_1$, $q_2$)

with two pressure drops ($\Delta P_1$, $\Delta P_2$). Hence, one steady-state experiment, at a given set of conditions (fixed $S_1$, $Ca$, $\kappa$, $\theta_e$, $Co$, $Bo$ etc.), does not provide sufficient information to determine the four coefficients. This difficulty has led many researchers to a quest for the design of experiments in which the coupling coefficient can be isolated (e.g., counter-current flow, etc). Such experiments can, indeed, prove the existence of strong coupling effects, but they can not be expected to yield the values of the coupling coefficients that pertain to steady-state co-current two-phase flow, given the large difference in the experimental conditions. Here, we develop a method which can determine these coefficients from a set of experiments of the same type (steady-state co-current two-phase flow) with rigorous statistical means. It is a parameter estimation method that obtains the functional dependence of the generalized coefficients in a global way by choosing the optimal functional representation of the unknown coefficients in order to match the experimental data with statistical rigor.

This method has the advantage that it uses only one set of experiments of the same type, which is both convenient and imperative. In this way, the experimental data are well controlled and correspond to the exact values of the parameters and to the flow mode and flow regimes which pertain to the flow system of interest. As will be seen below, the new method is simple and works very well.

The flow mechanisms and the macroscopic flow regimes affect the conventional relative permeabilities strongly (Avraam and Payatakes, 1995). In the past, the presumption has prevailed that the configuration of the fluids remains static under steady-state two-phase flow conditions. This, in turn, has led to a longstanding microconception concerning the mechanisms of the motion of the two phases. This assumption, which was first made by Richards (1931), presumes that a disconnected fluid cannot flow through the pore network, and, therefore, oil can flow only through connected pathways. On the other hand the oil (nonwetting fluid) is thought to be always disconnected below a certain saturation value (Honarpoor and Mahmood; 1988), in which case its permeability is thought to become nil. In Avraam and Payatakes (1994) it is shown that this dogma is not true (see also below), and in many actual situations of steady-state two-phase flow the disconnected parts of the fluids contribute substantially to the overall motion.

Avraam and Payatakes (1995) identified four main flow regimes: *large ganglion dynamics* (LGD), *small ganglion dynamics* (SGD), *drop traffic flow* (DTF) and *connected pathway flow* (CPF). Snapshots of such flows are given in Figure 1a–d. In the first two flow regimes, the motion of the oil is due to the dynamic process of ganglion motion, collision and coalescence, breakup, stranding and remobilization, leading to an overall dynamic equilibrium which was denoted as '*steady-state*' *ganglion dynamics*. The term 'steady-state' appears in quotation marks to show that the process is intrinsically a dynamic equilibrium of moving fluid parts, even though macroscopically it appears stable. Connected pathway flow for both fluids was observed only in the case of high flow rates. However, even in this case, elements of SGD and/or DTF were present in between the connected

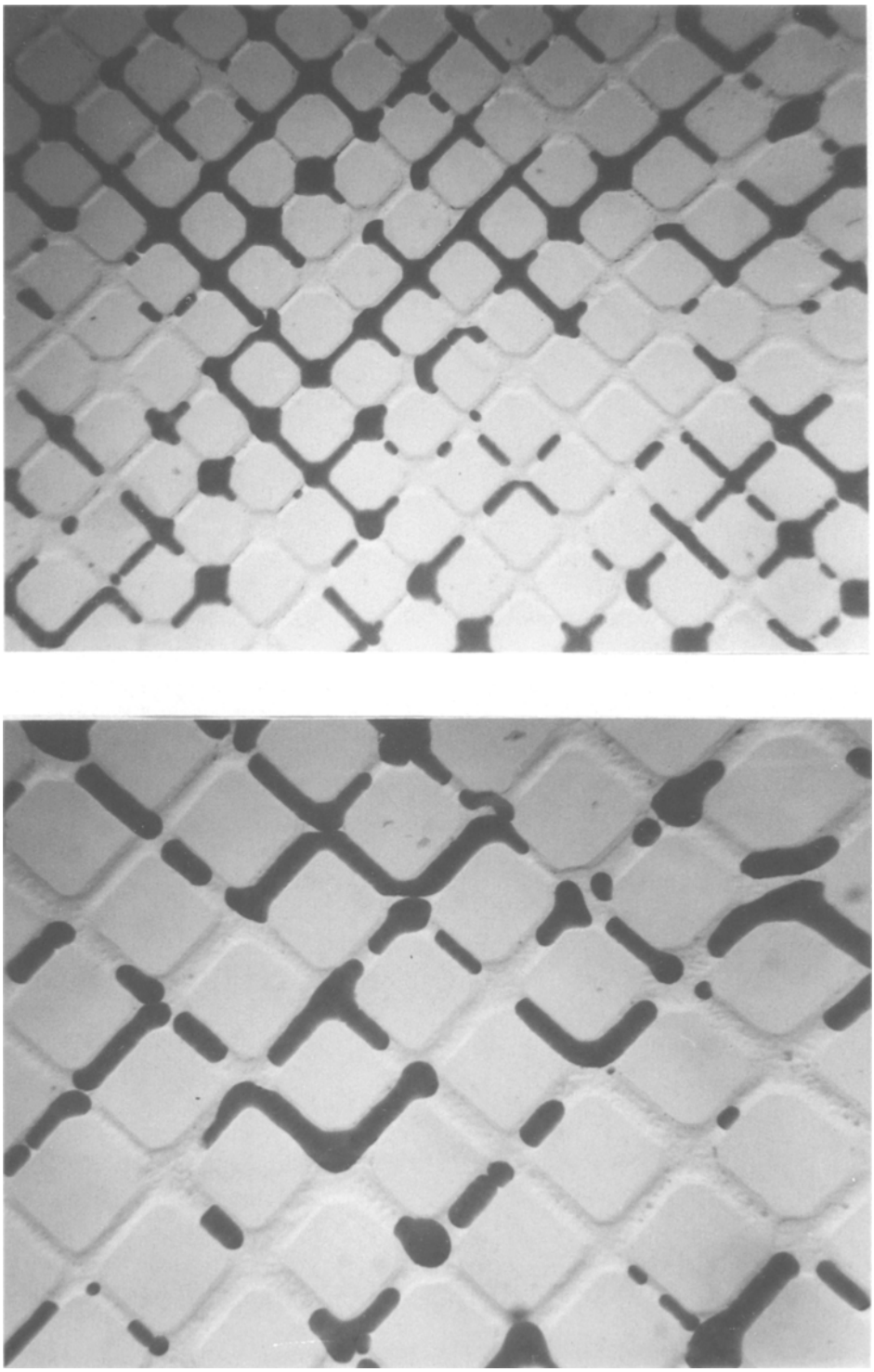

Fig. 1(a). Snapshots from steady-state two-phase flow experiments corresponding to the main flow regimes (a) Large ganglion dynamics (LGD). (1b) Small ganglion dynamics (SGD).

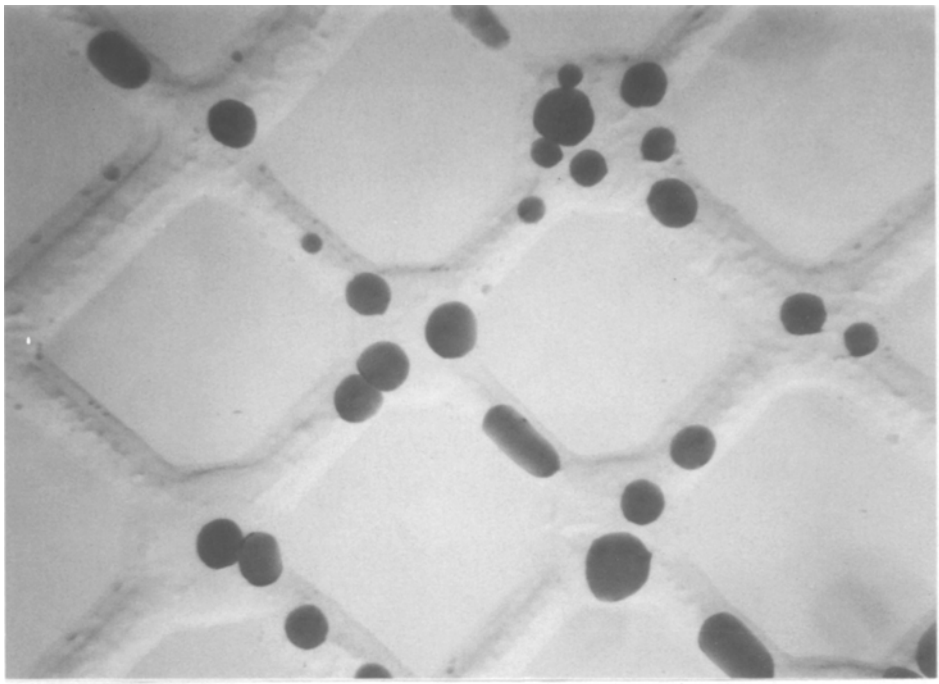

c

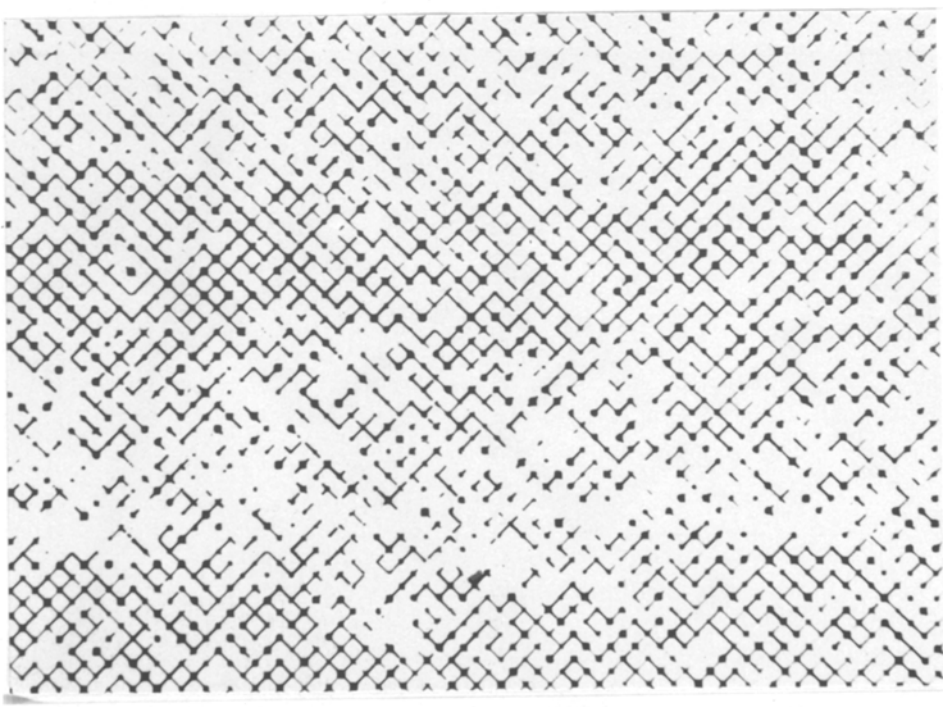

d

Fig. 1(c). Drop traffic flow (DTF) detail. (1d) Connected pathway flow (CPF). The snapshot shows the coexistence of connected pathway flow with small ganglion dynamics.

pathways, especially near the fringes of the oil pathways. The conventional relative permeabilities were found to correlate with the flow regimes strongly. The relative permeability to oil, $k_{r2}$, is minimal in the domain of LGD, and increases strongly as the flow mechanism changes from LGD to SGD to DTF to CPF. The relative permeability to water, $k_{r1}$, is minimal in the domain of SGD, and increases weekly as the flow mechanism changes from SGD to LGD, whereas it increases strongly as the mechanism changes from SGD to DTF to CPF.

To express the relative magnitude of the coupling effects, we define two new quantities, the *coupling indices*, as follows, $\chi_i \equiv 1-(k_{rii}/k_{ri})$. The experimentally determined values of the coupling coefficients were found to be correlated strongly with the flow regimes.

In steady-state two-phase flow the macroscopic pressure gradients in the two fluids are virtually equal, provided that the flow is fully developed (free from end-effects), because then the macroscopic gradient of the capillary pressure is nil. This is not only a theoretical expectation, based on the flow mechanisms, but also the result of careful experimental measurements (Bensten and Manai, 1993). In this case the coupling coefficients can be embedded in the conventional relative permeability coefficients, through the relations $[k^{\circ}_{ri} = k^{\circ}_{rii} + (\mu_i/\mu_j)k^{\circ}_{rij}; i, j = 1, 2; i \neq j]$. This can conceal the fact (and has done so many times in the past) that the coupling coefficients are important and that in many cases of practical interest they make the main contribution. The present work suggests a synthesis in the sense that one can use the conventional relative permeability coefficients to describe the macroscopic behaviour without losing sight of the fact that known and significant portions of their magnitudes (equal to the aforementioned coupling indices, $\chi_i$) are due to coupling effects. This synthesis applies strictly to steady-state co-current fully-developed flow; it does not apply to situations involving significant macroscopic gradients of the saturation and the capillary pressure, such as displacement fronts, etc.

## 3. Conventional and Generalized Relative Permeability Coefficient: A Review

The problem of the two-phase flow in porous media is usually treated with Darcy's extended law. For *horizontal, one-dimensional, immiscible, two-phase* flow in *homogeneous* and *isotropic* porous media, these equations take the form

$$v_1 = -\frac{kk_{r1}}{\mu_1}\frac{\Delta P_1}{L}, \tag{1a}$$

$$v_2 = -\frac{kk_{r2}}{\mu_2}\frac{\Delta P_2}{L}, \tag{1b}$$

where $k_{r1}$ and $k_{r2}$ are the conventional relative permeabilities for fluids 1 and 2, respectively, and $k$ is the absolute permeability of the porous medium. In these

equations, the interactions between the fluids are neglected and, therefore, the conventional relative permeabilities are thought (not rigorously) to represent the drag due to the flow of each particular fluid over the solid surface. In effect, it is assumed (arbitrarily) that the solid surface and each one of the fluids form a new porous matrix through which the other fluid can flow. This implies that all fluid–fluid *interfaces* remain *static* in steady-state flow, which is *not true.*

Once we accept that the fluid-fluid interfaces are not static, the interactions of the fluids become significant and the drag due to momentum transfer across the fluid-fluid interfaces should be taken into account. This gives rise to the viscous coupling effects. It has been shown theoretically that the magnitude of viscous coupling depends on the rheology of the oil–water interface, and it diminishes when the interfacial shear viscosity becomes significant (Ehrlich, 1993). The governing equations for *coupled immiscible two-phase* flow in *homogeneous* and *isotropic* porous media have been suggested by many authors (Raats and Klute, 1968; Rose, 1972; Shanchez-Palencia, 1974; Marle, 1982; de Gennes, 1983; de la Cruz and Spanos, 1983; Whitaker, 1986; Spanos *et al.*, 1986; Kalaydjian, 1987; Auriault, 1987; Auriault *et al.*, 1989) and their integrated form can be written as

$$v_1 = -\frac{kk_{r11}}{\mu_1}\frac{\Delta P_1}{L} - \frac{kk_{r12}}{\mu_2}\frac{\Delta P_2}{L}, \tag{2a}$$

$$v_2 = -\frac{kk_{r21}}{\mu_1}\frac{\Delta P_1}{L} - \frac{kk_{r22}}{\mu_2}\frac{\Delta P_2}{L}, \tag{2b}$$

where $k_{r11}$ and $k_{r22}$ are the generalized relative permeabilities for phases 1 and 2, respectively, and $k_{r12}$ and $k_{r21}$ are the viscous coupling coefficients.

The relative importance of the viscous coupling coefficients has been debated widely in the literature. The coupling coefficients are often assumed to be significant only when $\mu_1 = \mu_2$ and the saturation of one fluid is relatively low, but there is experimental evidence that the viscous coupling coefficients are also important when the fluid viscosities differ substantially (Kalaydjian and Legait, 1987; Goode and Ramakrishnan, 1993; also the present work). The coupling effects were reported to be insignificant in Yadav *et al.* (1987), where the conventional relative permeabilities of both phases remained unchanged during a drainage process when the opposite phase was solidified in situ. However, recent experimental studies (Kalaydjian *et al.*, 1989; Bourbiaux and Kalaydjian, 1988, 1990; Bentsen and Manai, 1993) have shown that the viscous coupling coefficients are indeed important and comparable to the diagonal coefficients.

Indirect but strong evidence that viscous coupling is important is that the conventional relative permeabilities depend on almost all the pertinent flow parameters. Besides the saturation and saturation history of the fluids (Johnson *et al.*, 1959; Naar *et al.*, 1962; Jerault and Salter, 1990) they also depend on the capillary number, $Ca$ (Leverett, 1939; Sandberg *et al.*, 1958; Taber, 1969; Lefebvre du Prey, 1973; Heavyside *et al.* 1982; Amaefule and Handy, 1982; Fulcher *et al.*, 1985),

the viscosity ratio $\kappa$ (Yuster, 1951; Odeh, 1959; Lefebvre du Prey, 1973), and the wettability characteristics, expressed here by the equilibrium contact angle $\theta_e$ (Owens and Archer, 1971; McCaffrey and Bennion, 1974; Morrow and McCaffery, 1978). Another important parameter is the coalescence factor, $Co$ (defined as the mean coalescence probability given a collision between two interfaces) (Constantinides and Payatakes, 1990). Avraam and Payatakes (1995) reported, for the first time, a strong correlation between the conventional relative permeabilities and the corresponding steady-state two-phase flow mechanisms.

The following conclusions can be drawn. If one insists on using the conventional fractional flow theory, then one should modify the approach by including the dependence of the relative permeabilities on all the pertinent parameters, i.e., for a given porous medium,

$$k_{ri} = k_{ri}(S_i; Ca, \kappa, \cos\theta_e, Co, \text{saturation history}, ...). \tag{3}$$

The fact that $k_1$ depends *strongly* on $Ca$, which is proportional to $v_1$, implies that the relation between $v_1$ and $\Delta P_1$ is strongly *nonlinear*, despite the fact that inertial effects are negligible under typical flooding conditions. The same holds true for $v_2$ and $\Delta P_2$. If, on the other hand, one intends to use the generalized fractional flow theory, one needs a reliable method to determine the non-diagonal terms, taking into account that the generalized relative permeability coefficients also depend on the parameters appearing in Equation (3),

$$k_{rij} = k_{rij}(S_i; Ca, \kappa, \cos\theta_e, Co, \text{saturation history}, ...). \tag{4}$$

Conventional relative permeabilities are measured in the laboratory with two basic methods: *unsteady-state flow* experiments (i.e. *immiscible displacement* experiments), and steady-state flow experiments.

The techniques used to estimate the conventional relative permeabilities from immiscible displacement data introduce many uncertainties. All techniques originate from the Buckley–Leverett theory (Buckley and Leverett, 1941; Rapoport and Leas, 1952). Those techniques, which are called explicit (Welge, 1952; Johnson *et al.*, 1959; Jones and Roszelle, 1978), calculate the point values of the conventional relative permeabilities directly from the measured data. However, they are subjected to significant errors (Tao and Watson, 1984). Implicit techniques may be used, instead. According to these techniques, a functional representation for the conventional relative permeabilities is chosen so that the effluent data evaluated by the mathematical model, with or without the capillary pressure, match the experimental data in a statistical sense. The functional representations may be simple equations with two parameters (Archer and Wong, 1973; Sigmund and McCaffery, 1979; Batycky *et al.*, 1981), but representations with cubic splines or B-splines are more flexible and reliable (Kerig and Watson, 1986; Watson *et al.*, 1988) and reduce significantly the bias error. The methods of estimating the unknown parametres can be simple trial-and-error adjustment (Archer and Wong, 1973), or general

nonlinear regression techniques. The latter permit the analysis of the variance error of the estimates and make possible the physical interpretation of them. Despite the sophistication of these techniques, it is highly debatable whether the concept of relative permeabilities can be applied rigorously in a narrow front involving steep and fuzzy gradients of saturation and pressure.

*Steady-state flow* experiments can be used to estimate conventional relative permeabilities much more reliably. The immiscible fluids flow simultaneously until saturation and pressure equilibrium is attained. This is usually time-consuming, which is a considerable disadvantage. Relative permeability data at various values of saturation are taken in a stepwise manner by adjusting the flowrate ratio appropriately, and this is also time-consuming. On the other hand, data produced by this method are more reliable because the saturations, fluid flow rates, and pressure gradients are all directly measured and correlated using Darcy's law. A suitable modification of the experimental method should also take into account the flow mechanisms and the pertinent flow parameters, as is suggested in Avraam and Payatakes (1995).

When one intends to determine generalized relative permeability coefficients from steady-state flow experiments, one set of experiments does not provide sufficient information for the unique determination of the four coefficients (Whitaker, 1986). A second set of experiments is necessary. Rose (1988) suggested that two sets of steady-state experiments, one without gravitational effects and another with gravitational effects, would provide sufficient data. However, this procedure is subject to great errors (Rose, 1989). Bourbiaux and Kalaydjian (1988) performed two sets of experiments, one with co-current two-phase flow with no capillary effects (i.e., with high flow rates) and another with countercurrent two-phase flow and null total flow, as it was first proposed by Lelievre (1966). They calculated the generalized coefficients by assuming that the viscous coupling coefficients were the same in the two types of experiments. A similar experimental procedure was followed by Kalaydjian (1990) in a square cross-section capillary tube and it was suggested for application in real porous media. However, this procedure is open to criticism because the two different injection modes (co-current and counter-current) produce different flow configurations, and the generalized permeability coefficients should be affected accordingly. In all these studies, the two coupling coefficients were taken equal to each other ($k_{r12}/\mu_2 = k_{r21}/\mu_1$), based on the assumption that the Osanger–Casimir reciprocity equation applies. Thus, only three coefficients had to be determined each time. This assumption needs to be discussed. In flow regimes such as 'steady-state' ganglion dynamics (Avraam and Payatakes, 1995), in which the motion of oil involves continual occurrence of *catastrophic pore-level flow events* (ganglion breakup, coalescence, stranding, mobilization), *microscopic reversibility does not exist*, and the Onsager–Casimir reciprocal relation should not be expected to hold. In Kalaydjian's experiments using square cross-section capillary tubes, catastrophic events were absent, and therefore his use of the reciprocity relation was justified. One, however, should not make this assumption in more

complex situations, such as those already mentioned. Indeed, Bentsen and Manai (1993) showed that the two off-diagonal viscous coupling coefficients are importants and not necessarily equal. The present work also shows that the off diagonal coefficients are very important and very unequal. A final comment is that to date only the dependence of the generalized coefficients on the fluid saturation has been studied. An extension including the rest of the flow parameters is warranted.

In this work, a proper combination of co-current steady-state two-phase flow experiments with a nonlinear parameter estimation method is suggested as a reliable and convenient means for the determination of all the necessary coefficients. The method has the advantage that one set of experiments (which are the same in nature with the flow process under consideration) is sufficient, and that the estimated coefficients can be endowed with a consistent physical interpretation. This gives the possibility, for the first time, to correlate all coefficients with the pertinent flow parameters, as well as with the underlying flow mechanisms.

## 4. Theory

### 4.1. PARAMETER ESTIMATION METHOD

In the context of the parameter estimation method, the dependent variables of the model under consideration are represented with a functional form,

$$\mathbf{y} = \mathbf{f}(\mathbf{x}; \boldsymbol{\theta}), \tag{5}$$

where $\mathbf{y}$ and $\mathbf{x}$ are the vectors of the dependent and the independent variables of the model, respectively, and $\boldsymbol{\theta}$ is the vector of the unknown parameters. A suitable experimental method provides the necessary measurements for both dependent and independent variables, $\mathbf{y}$ and $\mathbf{x}$. The measured values that correspond to the $\mu$th experiment and the $\alpha$th equation of the model are denoted by $y_{\mu\alpha}$ and $x_{\mu\alpha}$. The unknown parameters $\{\theta_i, i = 1, \ldots, N\}$, where $N$ is the total number of parameters in the model, are chosen so as to minimize the sum of the squares of the residuals,

$$e_{\mu\alpha} = y_{\mu\alpha} - f_{\mu\alpha}(\mathbf{x}_\mu; \boldsymbol{\theta}). \tag{6}$$

The sum of the squared residuals gives the objective function, which has the form

$$\Phi(\boldsymbol{\theta}) = [\mathbf{y} - \mathbf{f}(\mathbf{x}; \boldsymbol{\theta})]^T \mathbf{W} [\mathbf{y} - \mathbf{f}(\mathbf{x}; \boldsymbol{\theta})] = \mathbf{e}^T \mathbf{W} \mathbf{e}, \tag{7}$$

where $\mathbf{W}$ is a weighing matrix and $\mathbf{e}$ is the vector of the residuals, $e_{\mu\alpha}$.

The value of the parameter vector that minimizes the objective function, $\boldsymbol{\theta} = \boldsymbol{\theta}^*$, is called the estimator of the parameters. According to the selection of the weighing matrix, $\mathbf{W}$, the estimates of the parameters, $\boldsymbol{\theta}_i$, acquire certain desirable properties. If $\hat{\boldsymbol{\theta}}$ is the true (but unknown) value of the parameter vector, and we denote

with $\mathbf{V}$ the covariance matrix of the true errors, $\varepsilon_{\mu\alpha} = y_{\mu\alpha} - f_{\mu\alpha}(\mathbf{x}_\mu; \hat{\boldsymbol{\theta}})$, for all experiments and equations of the model, we can choose $\mathbf{W} = \mathbf{V}^{-1}$. Then the maximum-likelihood estimator is obtained, which maximizes the corresponding likelihood (Bard, 1974). Maximum likelihood estimators have important properties; they are consistent (i.e., asymptotically unbiased), and asymptotically efficient (i.e., as the number of the measurements increases beyond bound, the attainable covariance matrix of the estimator tends to a lower bound, given by the Rao–Cramer theorem).

Usually, the covariance matrix of the errors is not known, and some additional assumptions have to be made concerning the nature of the errors. If the errors are assumed to be independent and to have zero mean, the covariance matrix reduces to a diagonal matrix, whose elements are the variances of the errors. Then, the objective function takes the simpler form:

$$\Phi(\boldsymbol{\theta}) = \sum_{\alpha=1}^{a} \sum_{\mu=1}^{n} \frac{1}{\sigma_{\mu\alpha}^2} [y_{\mu\alpha} - f(\mathbf{x}_{\mu\alpha}; \boldsymbol{\theta})]^2 \tag{8}$$

where, $\sigma_{\mu\alpha}^2$ is the variance of the error in the $\mu$th experiment and in the $\alpha$th equation, a is the number of the model equations, and $n$ is the number of the available experimental measurements. A more general form could be obtained, if the covariance matrix of the errors were nondiagonal, but the simple form of the objective function in Equation (8) is sufficient for the estimation of the parameters.

Finally, if the variances of the diagonal covariance matrix are unknown, the stagewise maximization method can be used (Bard, 1974). According to this method, the unknown variances and the parameters are estimated simultaneously so as to minimize the objective function. The method can also be used when the covariance matrix of the errors has the general nondiagonal form.

The two models of the macroscopic equations of two-phase flow in porous media, i.e. the conventional one given by Equations (1a), (1b), and the generalized one given by Equations (2a), (2b), can be put directly in the form of Equation (5). We choose as independent variables the fluid pressure drops, $\Delta P_1$ and $\Delta P_2$, and the water saturation, $S_1$, and as dependent variables the superficial fluid velocities, $v_1$ and $v_2$, respectively. The functional representations of the conventional relative permeabilities and of the generalized relative permeability coefficients, written explicitly, should satisfy Equations (3) and (4). If we assume that the unknown covariance matrix of the errors is diagonal, the maximum likelihood estimator minimizes the following objective functions for the two models, respectively:

$$\begin{aligned} \Phi^{(1)}(\boldsymbol{\theta}) = & \sum_{\mu=1}^{n} \left\{ \left[ v_{1\mu} + \frac{k k_{r1}(S_{1\mu}; \boldsymbol{\theta})}{\mu_1} \Delta P_{1\mu} \right]^2 \right\} + \\ & + \sum_{\mu=1}^{n} \left\{ \left[ v_{2\mu} + \frac{k k_{r2}(S_{1\mu}; \boldsymbol{\theta})}{\mu_2} \Delta P_{2\mu} \right]^2 \right\} \end{aligned} \tag{9a}$$

and

$$\Phi^{(2)}(\boldsymbol{\theta}) = \sum_{\mu=1}^{n} \left\{ \left[ v_{1\mu} + \frac{kk_{r11}(S_{1\mu};\boldsymbol{\theta})}{\mu_1} \Delta P_{1\mu} + \frac{kk_{r12}(S_{1\mu};\boldsymbol{\theta})}{\mu_2} \Delta P_{2\mu} \right]^2 \right\} +$$

$$+ \sum_{\mu=1}^{n} \left\{ \left[ v_{2\mu} + \frac{kk_{r21}(S_{1\mu};\boldsymbol{\theta})}{\mu_1} \Delta P_{1\mu} + \frac{kk_{r22}(S_{1\mu};\boldsymbol{\theta})}{\mu_2} \Delta P_{2\mu} \right]^2 \right\}. \tag{9b}$$

In Equations (9a) and (9b) only the dependence of the coefficients $k_{ri}$ and $k_{rij}$ on $S_1$ (and of course on $\boldsymbol{\theta}$) is written explicitly. This is done to avoid cumbersome notation. The dependence of the coefficients on the rest of the flow parameters, $Ca, \kappa, \theta_e, Co$, saturation history, porous medium, etc., which is not explicitly written, has been considered separately. To this end, we made a parametric experimental study by changing systematically the values of $Ca$ and $\kappa$, while keeping the rest of the parameters constant. Then, the coefficients were estimated independently from each different set of experimental measurements obtained with a different set of $Ca$ and $\kappa$ values. The number of the experimental data available for each set of the flow parameters was either 5 (in most cases) or 4, as taken from Avraam and Payatakes 1995).

### 4.2. FUNCTIONAL REPRESENTATION OF THE TRANSPORT COEFFICIENTS

The problem of estimating the generalized relative permeability coefficients in Equations (9a) and (9b) is put in the form of a parameter estimation problem, when a suitable functional form is selected to represent the coefficients. By making the proper selection of the functional representation, one can minimize the total estimation error, which is composed of the bias error and the variance error. The former is due to the inability of the functional form to represent the true (albeit unknown) form of the coefficients, whereas the latter is due to the statistical uncertainty of the estimates caused by the inexact nature of the experimental measurements. Usually, a functional form with a great number of parameters decreases the bias error, since it is capable or representing a greater number of functions. On the other hand, it increases the variance error. A proper selection should minimize the total estimation error, which however is generally unknown.

Polynomial splines, or B-splines, are highly flexible functional forms which reduce drastically the bias error (Kerig and Watson, 1986). On the other hand, the variance error can be kept small through proper selection of the number of unknown parameters (Watson *et al.*, 1988). Here, we use cubic B-splines to represent the conventional relative permeabilities and the generalized relative permeability coefficients, and a suitable method in order to select the proper number of unknown parameters:

$$k_{ri} = \sum_{k=1}^{N} C_k^i \phi_k(S_1) \tag{10a}$$

and

$$k_{rij} = \sum_{k=1}^{N} C_k^{ij} \phi_k(S_1), \tag{10b}$$

where $C_k^i$ and $C_k^{ij}$ are the unknown parameters for $k_{ri}$ and $k_{rij}$, respectively, $\{\phi_k; k = 1, 2, \ldots, N\}$, are basic cubic B-splines, and $N$ is the number of the unknown parameters. For the sake of simplicity, we keep the same number of parameters for all coefficients, though this is not necessary.

By substituting Equations (10a) and (10b) in the objective functions (9a) and (9b), the parameters $C_k^i$ and $C_k^{ij}$ form the respective vectors $\boldsymbol{\theta}$, and the objective functions are to be minimized with respect to $\boldsymbol{\theta}$.

### 4.3. OPTIMIZATION METHOD

We used the standard Gauss–Marquardt method to minimize the objective functions (9a) and (9b). The method was found to be fast and stable. With four unknown parameters the method usually needed less than 100 iterative steps to converge.

Although it is always possible to find an (at least local) unconstrained minimum of the objective functions, the physical meaning of the coefficients requires that these coefficients should be positive. For this reason, the following linear inequality constraints are imposed:

$$k_{ri}(S_1, \boldsymbol{\theta}) \geqslant 0, \quad i = 1, 2 \tag{11a}$$

and

$$k_{rij}(S_1, \boldsymbol{\theta}) \geqslant 0, \quad i, j = 1, 2. \tag{11b}$$

For the problem of constrained minimization we used a projection method suitable for linear constraints. The projection method follows the Gauss–Marquardt minimization step whenever the coefficients are well inside the feasible region, whereas it follows the boundaries of the feasible region when a coefficient attempts to 'fall off'. In the latter case, a quadratic programming (QP) method is implemented, which performs constrained minimization of the local quadratic approximation of the objective function. The method uses the Kuhn–Tucker conditions (see Bard, 1974) to find the solution of the QP problem along the active constraints (i.e. constraints for which the equality holds locally). This also ensures the constrained minimization of the objective function, when the minimum is found to be on the boundaries of the feasible region. We found that the latter is not always the case, but in some cases the minimum is found inside the feasible region.

### 4.4. SELECTION OF THE APPROPRIATE NUMBER OF PARAMETERS

As the number of the unknown parameters increases the bias error (although unknown) decreases. On the other hand, the total number of parameters is limited

by the number of the available experimental measurements. The general rule is that the number of the experimental measurements must exceed the maximum number of unknown parameters per equation of the model, when the (diagonal) covariance matrix of the errors is unknown (Bard, 1970):

$$n > \max(l_\alpha). \tag{12}$$

In the present work and for a given set of conditions (fixed $Ca$, $\kappa$, etc.), we had $n = 5$ experimental measurements in the cases of $Ca = 10^{-7}$, $10^{-6}$, and $n = 4$ in the case of $Ca = 5 \times 10^{-6}$. For the sake of simplicity, all relative permeability coefficients were represented with four B-splines ($N = 4$). Such representations are simple and easy to handle. Thus, for the estimation of the conventional relative permeability coefficients, the number of the unknown parameters per equation was $l_\alpha = 4$, that is, one less than the number of the experimental measurements. For the case $Ca = 5 \times 10^{-6}$ we produced one additional artificial experimental measurement using the Aitken interpolation method. Such artificial data are known as interpolation data. For the estimation of the generalized coefficients, the number of the unknown parameters per equation was $l_\alpha = 8$. Using the Aitken method we produced four or five interpolation data points for $Ca = 10^{-7}$, $10^{-6}$ and $Ca = 5 \times 10^{-6}$ respectively, and the number of unknown parameters remained always one less than the number of the experimental measurements.

Figure 2a shows the convergence of the estimated conventional relative permeability coefficients, $k_{r1}$ and $k_{r2}$, when the number of parameters increases approaching that of the experimental measurements ($n = 5$). The estimated values improve from $N = 1$ to $N = 4$ and the objective function decreases as in Watson *et al.* (1988). When the number of parameters and experimental measurements are equal ($N = n = 5$) the parameter estimation is meaningless, since an exact solution of the model equations is possible. In that case the likelihood diverges.

The results of the estimation procedure, when interpolation data are produced for $n = 10$, 20, 40 and $N = 4$, are shown in Figure 2b. Figure 2c shows the results of the estimation procedure keeping the number of the experimental data the same as in Figure 2b but using $N = n - 1$. We observe that no appreciable improvement in the estimated values is achieved, which means that interpolation data are not necessary. The same holds for the generalized relative permeability coefficients; here, $n = 9$ experimental and interpolation data were sufficient for the estimation (see below, Figure 6).

## 5. Results and Discussion

### 5.1. EXPERIMENTAL APPARATUS AND PROCEDURE

A detailed description of the experimental apparatus and procedure is given in Avraam and Payatakes (1995). For the sake of self-sufficiency of the present work a brief description is given below.

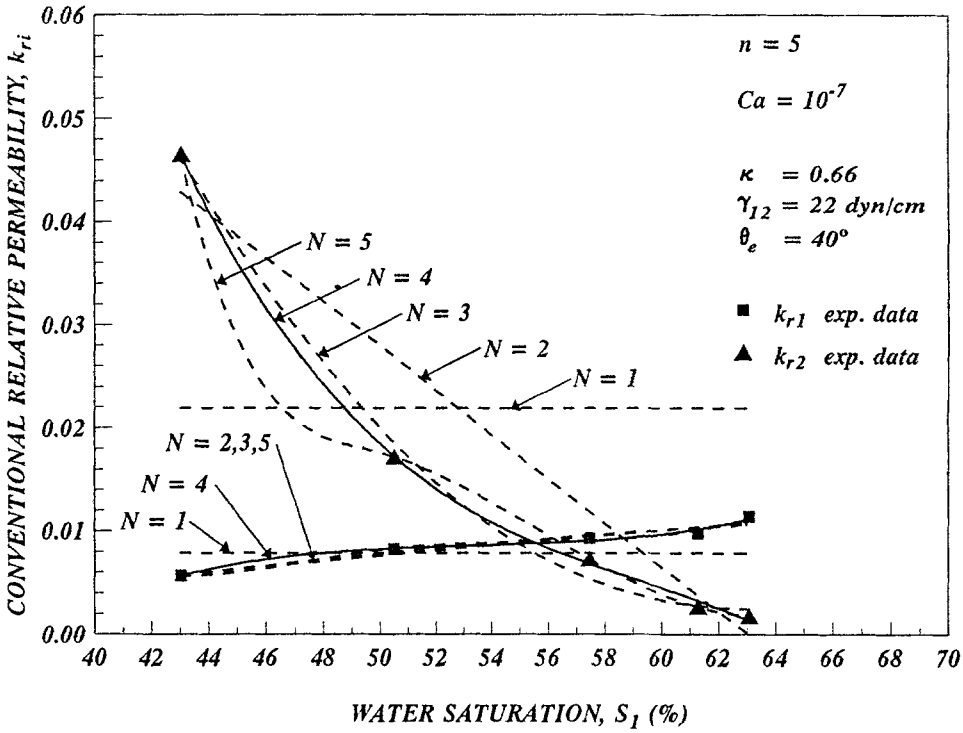


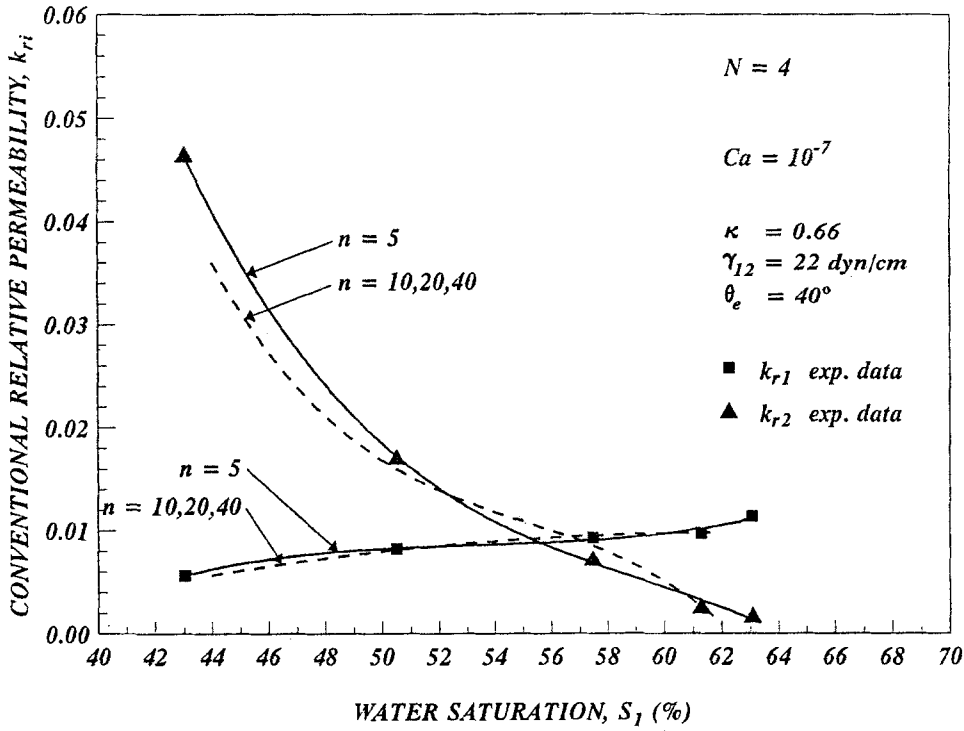


Fig. 2. Estimated curves of the conventional relative permeability coefficients, for a given set of flow conditions ($Ca = 10^{-7}$, $\kappa = 0.66$). (a) Dependence of the estimated curves on the number of parameters used in the B-spline representation of the coefficients. (b) Dependence of the estimated curves on the number of experimental data when interpolation data are added to the actual experimental measurements. The functional representation of the coefficients contains four parameters.

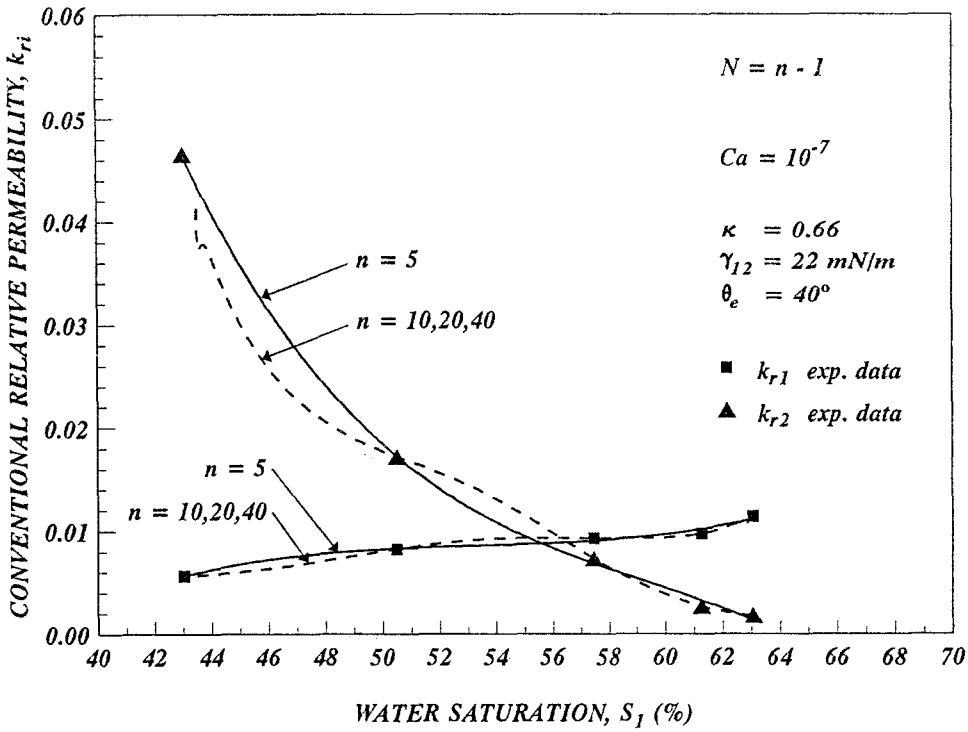


Fig. 2. (c) Same with b, but the functional representation of the coefficients contains one parameter less than the number of experimental data.

The model porous medium is a network of the chamber-and-throat type, etched in glass, and has characteristics that make it a relatively simple representation of a reservoir sandstone. It comprises 11 300 chambers and 22 600 throats. The mean values of the chamber and throat diameters are 560 $\mu$m and 112 $\mu$m, respectively, and the standard deviations of the populations are ca. 1/4 of the corresponding mean values. The maximum pore depth is nearly uniform and equal to ca. 140 $\mu$m. The node-to-node distance of the network is $l = 1221$ $\mu$m. At the beginning of each experiment the network is completely filled with the nonwetting liquid. Then, the two fluids are injected simultaneously with constant flowrates, using two syringe pumps, until steady-state is attained.

At steady-state measurements are made over a *central* region that covers ca. 1/4 of the entire network, to reduce the influence of end-effects. The pressure drop in each liquid is measured separately. This is achieved by placing suitable semipermeable membranes at the ends of the pressure taps for each of the two liquids. The pressure differences are monitored and recorded with a sensitive pressure transducer system, and the pressure signals are time-averaged to produce smooth, steady signals. The flow mechanisms are observed and videorecorded. The videorecorded signal is then digitized and processed with an image analyzer

to obtain the saturation values of the two fluids as functions of position and time. These data, in turn, are space-averaged and time-averaged to obtain the mean values of $S_1$ and $S_2$ corresponding to the conditions of the experiment. The end-effects do not significantly affect the details of the flow mechanisms in the region of measurements. This was verified by partitioning the region of measurements in six segments and by making statistical analysis of the time-averaged observations concerning the 'oil' (number of ganglia per unit area, ganglion size distribution) to check for any significant differences among the segments. None were found.

The data obtained in this way were processed to obtain the results presented below. It should be noted that the capillary number is calculated from $Ca = \mu_1 q_1/\gamma_{12} wl$, where $q_1$ is the flow rate of the 'water' and $w(= 70\,\text{mm})$ the width of the network.

### 5.2. FLOW REGIMES AND GENERALIZED RELATIVE PERMEABILITY COEFFICIENTS

Photographs of the main flow regimes of steady-state co-current two-phase flow are shown in Figures 1a–d. Figure 1a shows LGD (large ganglion dynamics), Figure 1b shows SGD (small ganglion dynamics), Figure 1c shows DTF (drop traffic flow), and Figure 1d shows CPF and SGD (connected pathway flow and SGD).

Figures 3, 4 and 5 present all the estimated values of the conventional (dashed lines) and generalized (solid lines) relative permeability coefficients as functions of the water saturation, $S_1$. Each figure corresponds to a constant value of the viscosity ratio, $\kappa = 0.66, 1.45, 3.35$, respectively (a fixed pair of immiscible fluids), whereas the capillary number, $Ca$, increased going from (a) to (c) and from $10^{-7}$ to $10^{-6}$ to $5 \times 10^{-6}$. The other flow parameters ($\theta_e$, $Co$, $Bo$, etc.) are kept constant. The flow regimes that correspond to the specific ranges of $S_1$ and $Ca$ are indicated (see also Figure 7).

The conventional and the generalized coefficients depend on the flow conditions and the corresponding flow mechanics. Summarizing, we can say that the conventional relative permeability coefficients, $k_{r1}$ and $k_{r2}$, are increasing functions of the saturation of the respective fluid, and they increase as $Ca$ and/or $\kappa$ increase. The generalized relative coefficient $k_{r12}$ increases with increasing $S_1$, whereas both $k_{r21}$ and $k_{r22}$ decrease with increasing $S_1$. The behavior of $k_{r11}$ is more complex. In most cases studied (Figures 3a, 3b, 4a, 5a, 5b, 5c) $k_{r11}$ increases as $S_1$ increases. However, in certain cases (Figures 3c, 4c) $k_{r11}$ decreases as $S_1$ increases, whereas in others (Figure 4b) it displays mixed behavior. As $Ca$ increases we can say, roughly, that all the generalized coefficients increase.

With regard to the flow of water, $k_{r11}$ is the dominant term in the domain of CPF, where it provides the main contribution to the conventional relative permeability $k_{r1}$. An exception to this is observed in the domain of CPF and SGD, at large $S_1$ values, where $k_{r12}$ becomes significant. This is an indication that the flow of the water is assisted by the motion of the numerous ganglia (and droplets) that move in

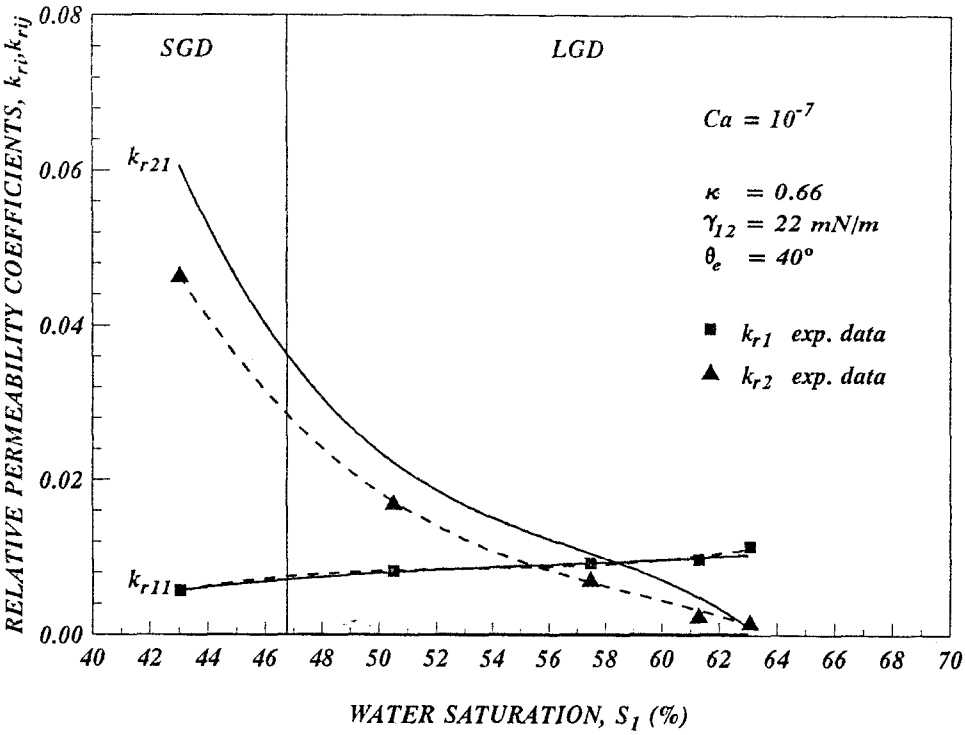
SGD
LGD
Ca = 10^-7
κ = 0.66
γ12 = 22 mN/m
θe = 40°
kr1 exp. data
kr2 exp. data
kr21
kr11
RELATIVE PERMEABILITY COEFFICIENTS, kri,krij
0.00
0.02
0.04
0.06
0.08
40 42 44 46 48 50 52 54 56 58 60 62 64 66 68 70
WATER SATURATION, S1 (%)

Fig. 3a.

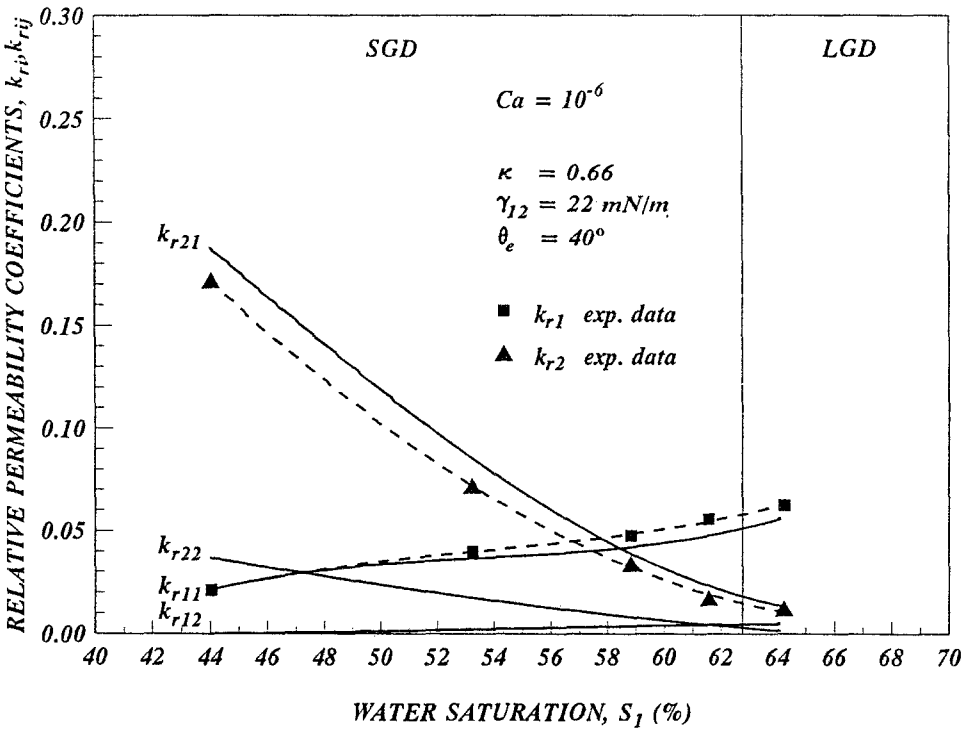
SGD
LGD
Ca = 10^-6
κ = 0.66
γ12 = 22 mN/m
θe = 40°
kr1 exp. data
kr2 exp. data
kr21
kr22
kr11
kr12
RELATIVE PERMEABILITY COEFFICIENTS, kri,krij
0.00
0.05
0.10
0.15
0.20
0.25
0.30
40 42 44 46 48 50 52 54 56 58 60 62 64 66 68 70
WATER SATURATION, S1 (%)

Fig. 3b.

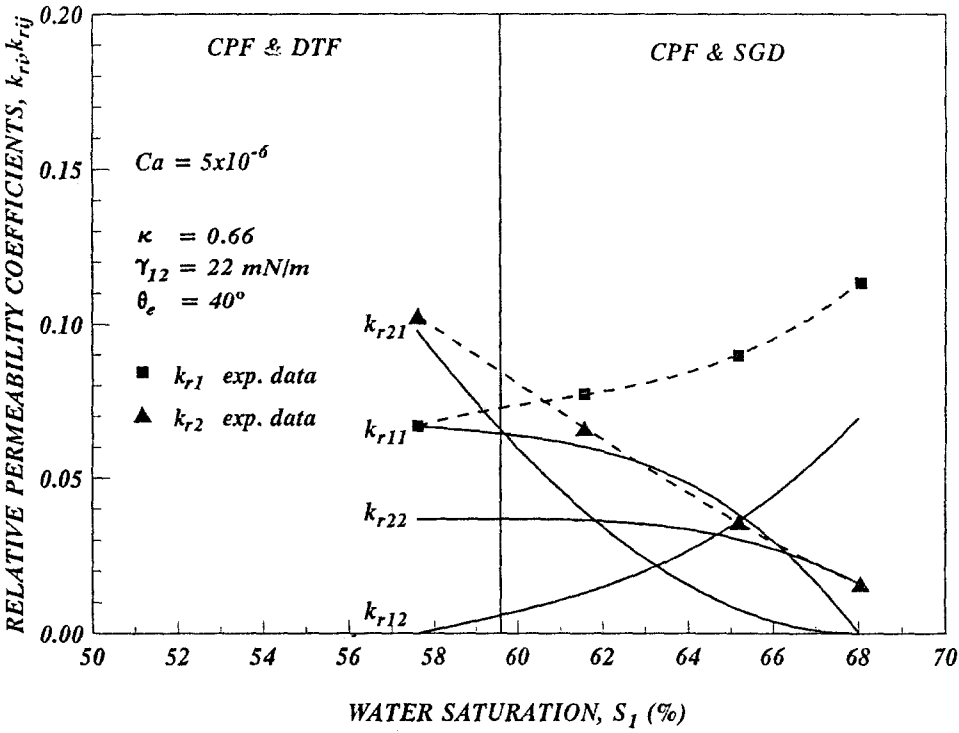


Fig. 3c.

Fig. 3. Conventional (dashed lines) and generalized (solid lines) relative permeability coefficients for $\kappa = 0.66$, with all the other physicochemical properties kept constant. (a) $Ca = 10^{-7}$, (b) $Ca = 10^{-6}$, (c) $Ca = 5 \times 10^{-6}$.

the water pathways, especially along the fringes of the connected oil pathways. In the domains of steady-state ganglion dynamics (LGD, SGD) the behavior is more complex. For $\kappa < 1$, the coefficient $k_{r11}$ makes the dominant contribution, even though $k_{r12}$ is discernible. For $\kappa > 1$ the coefficient $k_{r11}$ becomes less significant, and $k_{r12}$ becomes large, even dominant. This is strong evidence that the flow of the water is assisted considerably by the flow of the population of moving ganglia. This phenomenon is enhanced slightly as $S_2$ increases ($S_1$ decreases).

A significant result concerning the flow of the oil is that in the domains of LGD, SGD and DTF, where the oil is disconnected, $k_{r21}$ is often nearly equal to the conventional relative permeability, $k_{r2}$ (Figs. 3, 4, 5), whereas $k_{r22}$ is small or nil. This shows the crucial importance of the coupling effects. In these cases the motion of the disconnected oil is caused mainly by the flowing water. The diagonal term $k_{r22}$ becomes significant only at high oil saturation, $S_2$, especially in the domain of CPF and SGD, or CPF and DTF. In the latter case, the main contribution to the overall flow rate is that of the connected oil pathways, while the ganglia and/or droplets that move along the fringes of the oil pathways contribute to a smaller but still appreciable extent.

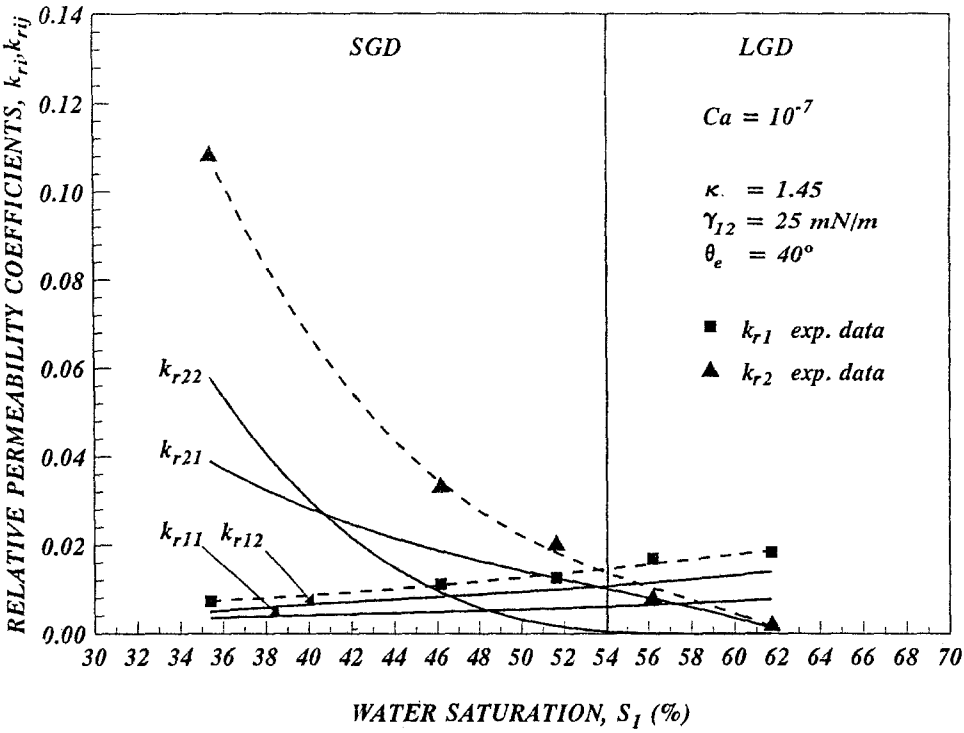
SGD
LGD
Ca = 10^-7
κ = 1.45
γ12 = 25 mN/m
θe = 40°
kr1 exp. data
kr2 exp. data
kr22
kr21
kr11
kr12
RELATIVE PERMEABILITY COEFFICIENTS, kri,krij
WATER SATURATION, S1 (%)

Fig. 4a.

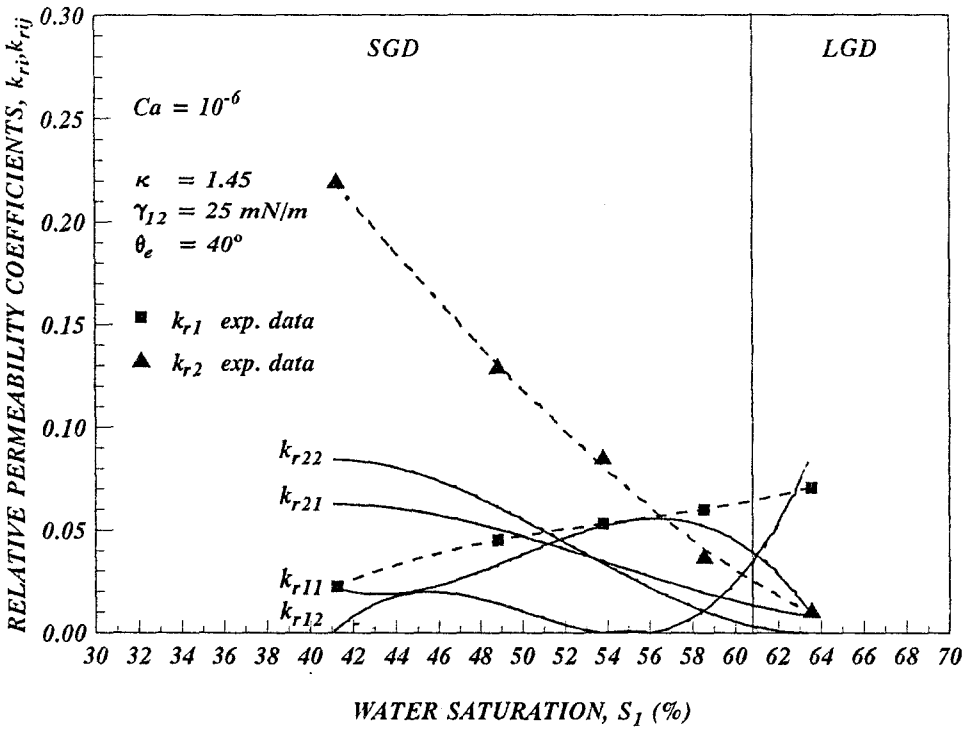
SGD
LGD
Ca = 10^-6
κ = 1.45
γ12 = 25 mN/m
θe = 40°
kr1 exp. data
kr2 exp. data
kr22
kr21
kr11
kr12
RELATIVE PERMEABILITY COEFFICIENTS, kri,krij
WATER SATURATION, S1 (%)

Fig. 4b.

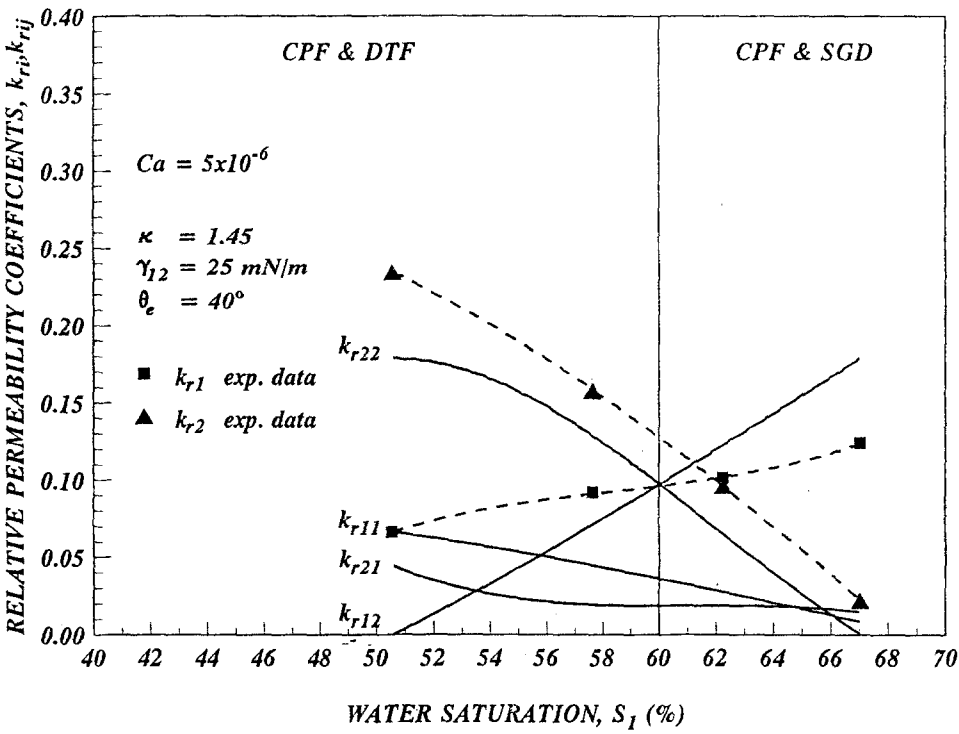


Fig. 4c.

Fig. 4. Conventional (dashed lines) and generalized (solid lines) relative permeability coefficients for $\kappa = 1.45$, with all the other physicochemical properties kept constant. (a) $Ca = 10^{-7}$, (b) $Ca = 10^{-6}$, (c) $Ca = 5 \times 10^{-6}$.

### 5.3. FLOW REGIMES AND COUPLING INDICES

The relative importance of the coupling effects can be expressed appropriately through the coupling indices, $\chi_i$, which are introduced here as

$$\chi_i = 1 - \frac{k_{rii}}{k_{ri}}, \quad i = 1, 2. \tag{13}$$

The coupling index, $\chi_i$, is the fraction of the flow rate of fluid $i$ that is caused by coupling effects. An alternative expression for $\chi_i$ is

$$\chi_i = \frac{\mu_i}{\mu_j} \frac{k_{rij}}{k_{ri}} \left( \frac{\Delta P_j}{\Delta P_i} \right), \quad i, j = 1, 2, \quad i \neq j. \tag{14}$$

Equation (14) follows from a simple expression that relates the conventional and generalized coefficients, and which is obtained by combining Equations (1) and (2).

$$k_{ri} = k_{rii} + \frac{\mu_i}{\mu_j} k_{rij} + \frac{\mu_i}{\mu_j} k_{rij} \frac{\Delta P_j - \Delta P_i}{\Delta P_i} = k_{rii} + \frac{\mu_i}{\mu_j} k_{rij} \frac{\Delta P_j}{\Delta P_i},$$

$$i, j = 1, 2, \quad i \neq j. \tag{15}$$

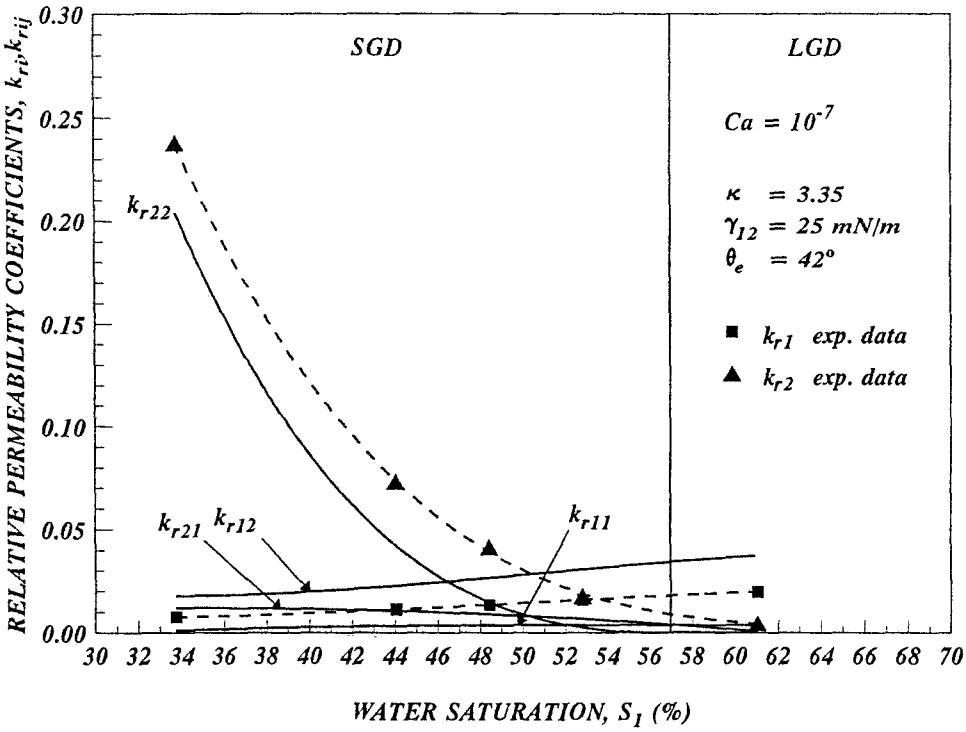
SGD
LGD
Ca = 10^-7
κ = 3.35
γ12 = 25 mN/m
θe = 42°
kr1 exp. data
kr2 exp. data
kr22
kr21
kr12
kr11
RELATIVE PERMEABILITY COEFFICIENTS, kri,krij
WATER SATURATION, S1 (%)

Fig. 5a.

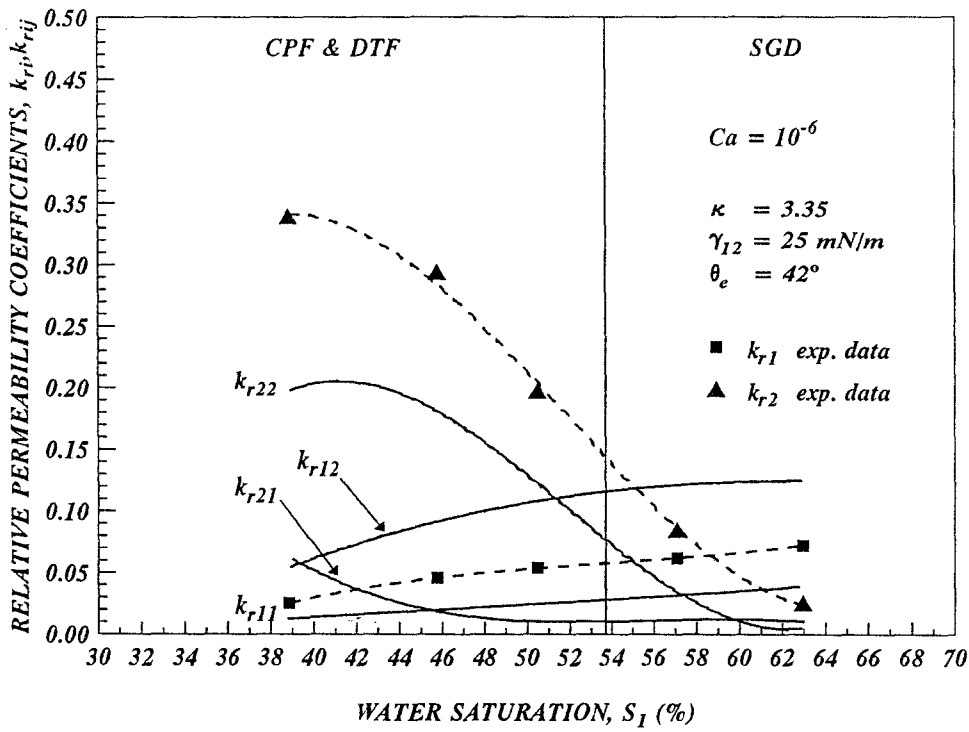
CPF & DTF
SGD
Ca = 10^-6
κ = 3.35
γ12 = 25 mN/m
θe = 42°
kr1 exp. data
kr2 exp. data
kr22
kr12
kr21
kr11
RELATIVE PERMEABILITY COEFFICIENTS, kri,krij
WATER SATURATION, S1 (%)

Fig. 5b.

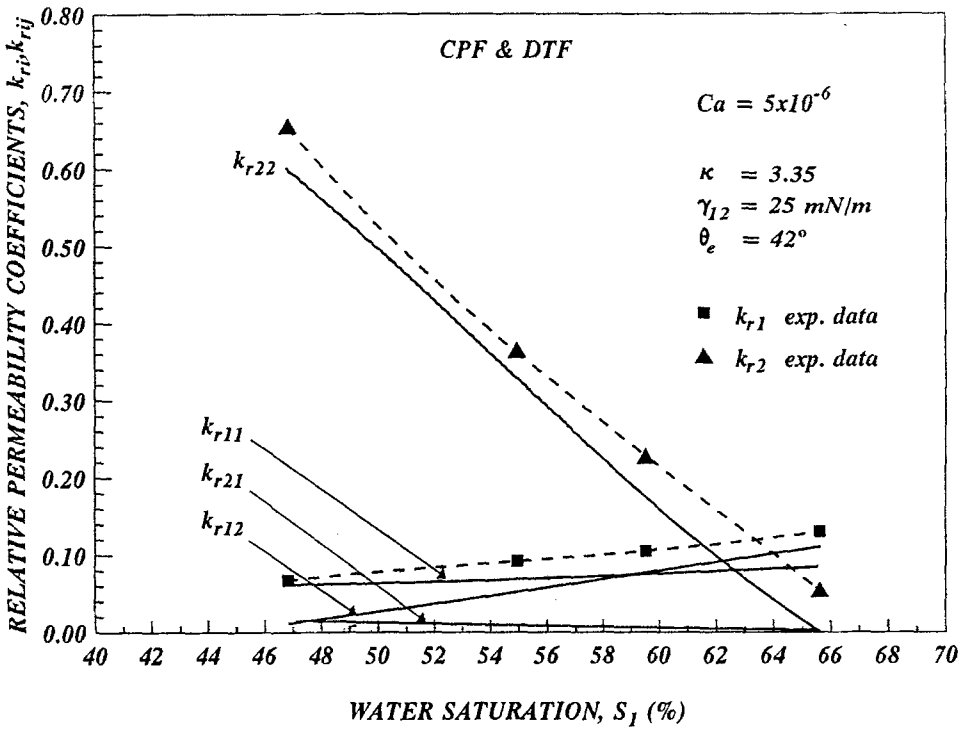


Fig. 5c.

Fig. 5. Conventional (dashed lines) and generalized (solid lines) relative permeability coefficients for $\kappa = 3.35$, with all the other physicochemical properties kept constant. (a) $Ca = 10^{-7}$, (b) $Ca = 10^{-6}$, (c) $Ca = 5 \times 10^{-6}$.

The combination of the two models is permissible here because the experimental data utilized by the method correspond not only to the same flow rates and pressure drops but also (a condition that is very important) to the same type of flow (steady-state, co-current), and the same flow regimes. For fully developed flow in an infinite porous medium, which is free from end and boundary effects, we have $\Delta P_i = \Delta P_j$, and Equations (15) and (14) reduce to

$$k_{ri}^{\circ} = k_{rii}^{\circ} + \frac{\mu_i}{\mu_j} k_{rij}^{\circ}, \quad i, j = 1, 2, \quad i \neq j \tag{16}$$

and

$$\chi_i^{\circ} = 1 - \frac{k_{rii}^{\circ}}{k_{ri}^{\circ}} = \frac{\mu_i}{\mu_j} \frac{k_{rij}^{\circ}}{k_{ri}^{\circ}}, \quad i, j = 1, 2, \quad i \neq j, \tag{17}$$

where the supersript $^{\circ}$ denotes quantities that are free from end and boundary effects. Laboratory experiments that are entirely free from end-effects are very difficult to achieve. However, in the present work we take advantage of the small but discernible end effects and, thus, turn a small disadvantage to a desirable feature.

TABLE I. Application of Wald's criterion[a] for model discrimination

| $R$ =Ratio of Model 1 to Model 2 likelihood values | $Ca = 10^{-7}$ | $Ca = 10^{-6}$ | $Ca = 5 \times 10^{-6}$ |
|---|---|---|---|
| $\kappa = 0.66$ | 1130 | 266 | 0.0413 |
| $\kappa = 1.45$ | 19.8 | 6.49 | 0.5790 |
| $\kappa = 3.35$ | 32.9 | 6.53 | 0.0018 |

Model 1: Conventional fractional flow model.
Model 2: Generalized fractional flow model.
At confidence level 95%:
- if $R \geqslant 19.0$ Model 1 is superior.
- if $R \leqslant 0.0526$ Model 2 is superior.
- if $0.0526 < R < 19.0$ more experiments are required to decide this issue.

[a] See Bard (1974).

It is this small difference ($\Delta P_1 \neq \Delta P_2$ but $|\Delta P_1 - \Delta P_2| \ll |\Delta P_1|$) that allows us to use Equation (15) rather than (16), and thus to determine the coupling effect contributions. When Equation (16) holds exactly, one cannot isolate the coupling effects from the overall behavior, because the RHS of Equation (16) functions as a single coefficient. This point requires elaboration.

It is important to understand that the coupling effects are *not* created by the end-effects. Rather, the small perturbation caused by the end-effects provides sufficient differentiation (ca. 10%) between the two pressure-drop signals to allow a statistically significant *decoupling* of the composite parameters $[k^{\circ}_{rii} + (\mu_i/\mu_j)k^{\circ}_{rij}]$. The weak end-effects under consideration do *not* significantly affect the details of the *flow mechanisms* in the region of the porous medium over which measurements were made. This was confirmed as follows. The region of measurements was partitioned in six segments, the flow behavior (number of ganglia per unit area, ganglion size distribution) was videorecorded and digitized and a statistical analysis was made to detect any significant differences between the time-averaged results among the six compartments. None were found. Thus, the coupling effects must be attributed to the flow mechanisms. It is also pertinent to point out that in the case of 'infinitely long' porous media sufficient perturbation to differentiate the two pressure gradient signals can be introduced by a *slight* local or (spatially periodic) variation of the mean pore diameter (or of the wettability) on a mesoscopic scale.

Figure 6 shows the application of both Equationss (16) and (15) to one of the cases in which the generalized coefficients have been estimated. Dashed lines present the results of Equation (16), whereas solid lines present those of Equation (15). The dotted lines are the estimated conventional relative permeabilities. Clearly, Equation (15) gives a sigificantly better approximation to the conventional

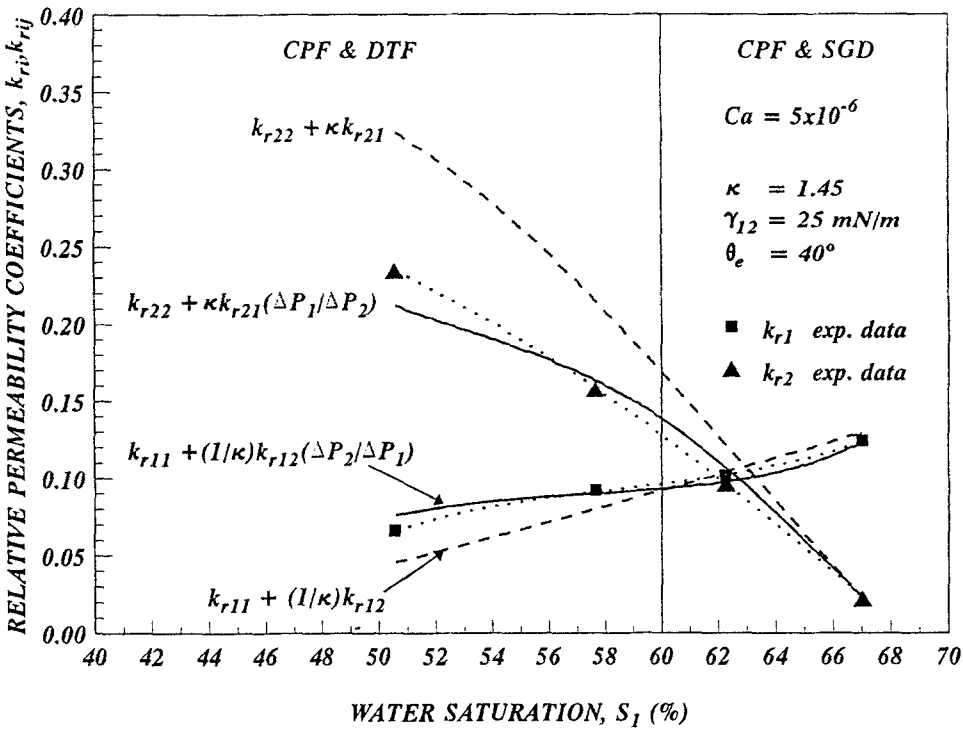


Fig. 6. Illustration of the simple relationship between the conventional and the generalized relative permeability coefficients for one set of flow conditions ($Ca = 5 \times 10^{-6}, \kappa = 1.45$). The estimated curves of the conventional relative permeability coefficients are presented with dotted lines.

permeabilities, because in these experiments there exist weak but discernible end effects, and $\Delta P_i \neq \Delta P_j$.

Figure 7 shows the coupling indices that were determined in this work and the map of the flow regimes, which was obtained in Avraam and Payatakes (1995). It should be kept in mind that because of the way in which the coupling coefficients, $\chi_i$, are calculated from the relative permeability coefficients $k_{ri}$ and $k_{rii}$, Equation (13), the relative error of $\chi_i$ is roughly equal to the sum of the relative errors of $k_{ri}$ and $k_{rii}$. Consequently, the values of $\chi_1$ and $\chi_2$ shown in Figure 7, and tabulated in Table II, should be considered as rough approximations. Still, certain important conclusions can be drawn.

The coupling index of oil, $\chi_2$, is large almost everywhere; it diminishes only near the domain of CPF, especially for $\kappa > 1$. In the domain of LGD and SGD, $\chi_2$ is large (in many cases near unity), and it is, in general, an increasing function of $S_1$ (decreasing function of $S_2$). These results are strong evidence that the bodies of disconnected oil (ganglia, droplets) are driven to a large extent by the flowing water that engulfs them. However, the fact that $\chi_2$ is usually less than unity indicates that ganglion-ganglion interactions make a sizable contribution. Such oil–oil interactions are observed frequently in our experiments. For example, when a moving ganglion collides with another slowly moving ganglion, the pair (even if

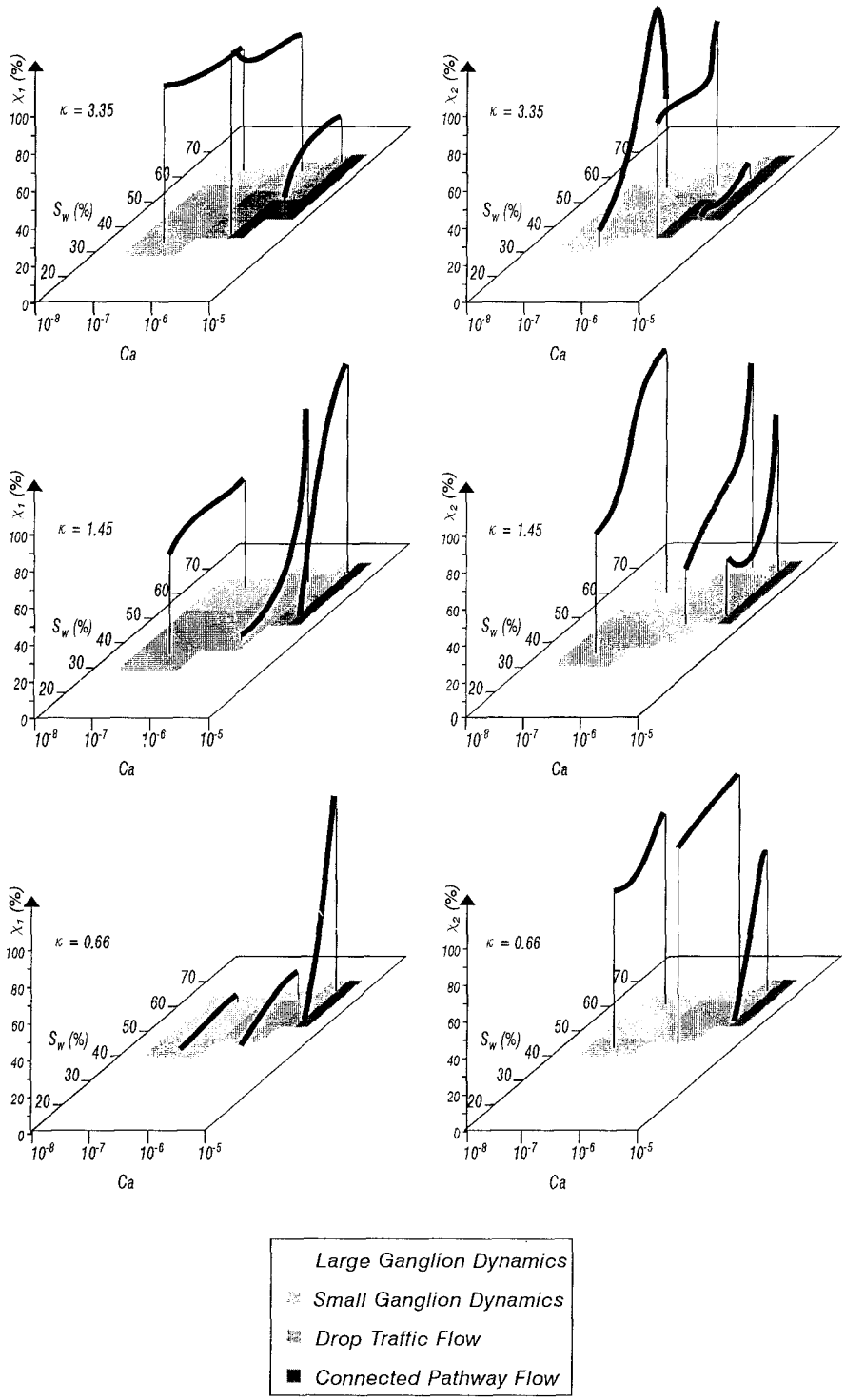


Fig. 7. Map of flow regimes and estimated coupling indices. The graph shows a strong correlation between the coupling indices and the flow regimes. For discussion see the text.

TABLE IIa. Estimated values of the conventional relative permeabilities, $k_{r1}, k_{r2}$, and the coupling indices, $\chi_1, \chi_2$

$Ca = 10^{-6}$

$\kappa = 3.35$

| $S_1(\%)$ | $k_{r1}(\%)$ | $k_{r2}(\%)$ | $\chi_1(\%)$ | $\chi_2(\%)$ |
|---|---|---|---|---|
| 60.9 | 1.97 | 0.44 | 56.52 | 66.92 |
| 52.8 | 1.60 | 1.90 | 57.28 | 129.79 |
| 48.4 | 1.36 | 3.93 | 58.39 | 76.55 |
| 44.0 | 1.11 | 7.40 | 60.50 | 47.99 |
| 33.7 | 7.59 | 23.80 | 70.40 | 16.89 |

$\kappa = 1.45$

| $S_1(\%)$ | $k_{r1}(\%)$ | $k_{r2}(\%)$ | $\chi_1(\%)$ | $\chi_2(\%)$ |
|---|---|---|---|---|
| 61.7 | 1.87 | 0.17 | 51.63 | 110.48 |
| 56.2 | 1.58 | 1.03 | 50.19 | 111.50 |
| 51.6 | 1.34 | 1.84 | 51.11 | 99.29 |
| 46.2 | 1.10 | 3.41 | 52.41 | 79.09 |
| 35.4 | 7.36 | 10.90 | 46.57 | 51.88 |

$\kappa = 0.66$

| $S_1(\%)$ | $k_{r1}(\%)$ | $k_{r2}(\%)$ | $\chi_1(\%)$ | $\chi_2(\%)$ |
|---|---|---|---|---|
| 63.0 | 1.110 | 0.141 | 2.84 | 81.56 |
| 61.3 | 1.020 | 0.324 | 3.02 | 80.05 |
| 57.5 | 0.905 | 0.679 | 2.83 | 79.66 |
| 50.5 | 0.830 | 1.720 | 1.19 | 76.57 |
| 43.0 | 0.564 | 4.650 | 0.00 | 72.14 |

the ganglia do not coalesce) moves faster than the slower of the two ganglia before the collision. Another effect is the mobilization of stranded ganglia by oncoming moving ganglia.

The coupling index of water, $\chi_1$, is also substantial in most cases, with some exceptions. In the domain near CPF and for $\kappa = 3.35$, $\chi_1$ becomes small, especially for small values of $S_1$. In the domains of LGD and SGD, and for $\kappa < 1$, $\chi_1$ is small, even nil. It is also evident that $\chi_1$ is larger when $\kappa > 1$, than it is when $\kappa < 1$. This can be explained by the fact that the moving portions of oil exert larger viscous stresses on the water, as the oil viscosity increases, all other factors being the same. The peaks observed in the domain CPF and SGD for large $S_1$ (small $S_2$) values are attributed to the fact that in this flow regime a substantial amount of water is carried

TABLE IIb. Estimated values of the conventional relative permeabilities, $k_{r1}, k_{r2}$, and the coupling indices, $\chi_1, \chi_2$

$Ca = 10^{-6}$

$\kappa = 3.35$

| $S_1(\%)$ | $k_{r1}(\%)$ | $k_{r2}(\%)$ | $\chi_1(\%)$ | $\chi_2(\%)$ |
|---|---|---|---|---|
| 62.9 | 7.19 | 2.42 | 53.38 | 86.40 |
| 57.1 | 6.21 | 8.55 | 55.44 | 59.92 |
| 50.5 | 5.37 | 20.50 | 58.73 | 61.08 |
| 45.8 | 4.59 | 28.50 | 63.30 | 59.93 |
| 38.9 | 2.54 | 34.10 | 66.73 | 59.33 |

$\kappa = 1.45$

| $S_1(\%)$ | $k_{r1}(\%)$ | $k_{r2}(\%)$ | $\chi_1(\%)$ | $\chi_2(\%)$ |
|---|---|---|---|---|
| 63.5 | 7.04 | 1.03 | 81.50 | 96.99 |
| 58.5 | 6.02 | 4.14 | 32.61 | 68.99 |
| 53.8 | 5.31 | 8.16 | 16.34 | 62.37 |
| 48.8 | 4.50 | 13.20 | 11.76 | 55.69 |
| 41.2 | 2.29 | 21.90 | 2.19 | 41.33 |

$\kappa = 0.66$

| $S_1(\%)$ | $k_{r1}(\%)$ | $k_{r2}(\%)$ | $\chi_1(\%)$ | $\chi_2(\%)$ |
|---|---|---|---|---|
| 64.2 | 6.26 | 1.10 | 11.84 | 83.40 |
| 61.6 | 5.48 | 1.90 | 12.19 | 80.24 |
| 58.8 | 4.84 | 3.24 | 11.68 | 79.85 |
| 53.2 | 3.97 | 7.23 | 8.24 | 78.32 |
| 44.0 | 2.10 | 17.20 | 0.00 | 72.14 |

along in the form of films and piston-like segments formed among neighboring small ganglia.

Application of Wald's criterion (Bard, 1974) for model discrimination (Table I) shows that Model 1 (without coupling terms) is superior to Model 2 (with coupling terms) in the domain of steady-state ganglion dynamics, at a confidence level of 95 %. In the domain of connected pathway flow the two models are virtually equivalent, at a confidence level of 95 %, with a slight (but not always statistically significant) superiority of Model 2.

## 6. Conclusions

A reliable and easy to use method for the determination of the generalized relative permeability coefficients from a set of steady-state co-current two-phase flow data

TABLE IIc. Estimated values of the conventional relative permeabilities, $k_{r1}, k_{r2}$, and the coupling indices, $\chi_1, \chi_2$

$Ca = 5 \times 10^{-6}$

$\kappa = 3.35$

| $S_1(\%)$ | $k_{r1}(\%)$ | $k_{r2}(\%)$ | $\chi_1(\%)$ | $\chi_2(\%)$ |
|---|---|---|---|---|
| 65.5 | 13.00 | 5.70 | 25.37 | 10.32 |
| 59.5 | 10.50 | 23.00 | 27.47 | 2.65 |
| 55.0 | 9.22 | 36.10 | 24.35 | 0.26 |
| 46.8 | 6.71 | 65.50 | 8.93 | 2.78 |

$\kappa = 1.45$

| $S_1(\%)$ | $k_{r1}(\%)$ | $k_{r2}(\%)$ | $\chi_1(\%)$ | $\chi_2(\%)$ |
|---|---|---|---|---|
| 67.0 | 12.40 | 2.32 | 99.56 | 92.50 |
| 62.3 | 10.20 | 9.55 | 83.16 | 28.55 |
| 57.6 | 9.10 | 15.90 | 53.51 | 17.69 |
| 50.6 | 6.63 | 23.40 | 0.00 | 27.39 |

$\kappa = 0.66$

| $S_1(\%)$ | $k_{r1}(\%)$ | $k_{r2}(\%)$ | $\chi_1(\%)$ | $\chi_2(\%)$ |
|---|---|---|---|---|
| 68.0 | 11.30 | 1.61 | 93.92 | 63.28 |
| 65.2 | 9.02 | 3.55 | 60.98 | 38.84 |
| 61.6 | 7.71 | 6.61 | 25.74 | 14.28 |
| 57.6 | 6.69 | 10.20 | 0.00 | 0.00 |

was developed. It is a parameter estimation method that obtains the functional dependence of the generalized coefficients in a global way, by choosing the optimal functional representation of the unknown coefficients in order to match the experimental data with statistical rigor. The same method can also be used to obtain the conventional relative permeabilities. This method has the fundamental advantage that it uses data from flows that are of the *same nature* with that of the flow under consideration, namely, steady-state co-current two-phase flow. This is both convenient and imperative, since the nature of the flow affects every flow-related quantity, including the values of the relative permeabilities and the magnitude of the coupling effects.

The new method was used to analyze the flow data from the parametric experimental investigation of steady-state co-current two-phase flow that was reported in Avraam and Payatakes (1995). The main conclusions are the following.

- The viscous coupling effects are important over broad ranges of the values of the flow parameters $S_1, Ca, \kappa$, keeping all other factors (wettability, coalescence factor, porous medium) fixed.
- The cross coefficients in Equations (2a) and (2b) are found to be *unequal*, $k_{r12}/\mu_2 \neq k_{r21}/\mu_1$. For the class of flows under consideration this is *not* a violation of the Onsager–Casimir reciprocity relation, because the underlying flow mechanisms involve many *catastrophic* events (ganglion breakup, coalescence, stranding, mobilization), and therefore *do not possess microscopic reversibility.* (The Onsager–Casimir reciprocal relations hold only for phenomena that have microscopic reversibility.)
- The relative importance of the coupling effects is expressed appropriately through the *coupling indices*, which are introduced here, and which are defined as $\chi_i = 1 - (k_{rii}/k_{ri})$. These indices take values in the range (0, 1) and each of them is the normalized measure of the contribution of coupling effects to the flow rate of the corresponding fluid.
- The coupling indices are found to correlate strongly with the flow regimes, Fig. 7. These experimental results are in accord with the underlying flow mechanisms at pore level, and this provides a substantial insight into the process. It is established, among other things, that the bodies of disconnected oil (ganglia and droplets) are driven mainly by the flowing water that engulfs them. However, interactions between colliding bodies of oil are also significant. More detailed discussion of these issues is given in the main part of this work.
- A strikingly simple relationship is established between the generalized relative permeability coefficients and the conventional ones, specifically, Equation (15). In fully development flows (free of end and boundary effects) it is $\Delta P_j/\Delta P_i = 1$, and the above expression reduces to Equation (16). This relation explains the reason for which the coupling effects are so hard to isolate through macroscopic measurements; they are incorporated seamlessly in the values of $k_{ri}$. In the present work their isolation became possible because the data contained small but discernible differences between $\Delta P_1$ and $\Delta P_2$, caused by weak end-effects. *The coupling effects are inherent in the flow.* The weak end-effects made it possible to differentiate the two pressure drop signals, and thus to decouple the composite parameters $[k^{\circ}_{rii} + (\mu_i/\mu_j)k^{\circ}_{rij}]$ in a statistically significant way. [In 'infinitely long' porous media this can be achieved by introducing slight local perturbations in the mean pore diameter (or the wettability, etc.) on a mesoscopic scale.]
- Based on Wald's criterion for model discrimination (at a confidence level of 95 %) the conventional fractional flow model (no coupling effects) is superior to the generalized fractional flow model (with coupling effects) in the domain of steady-state ganglion dynamics. In the domain of connected pathway flow the two models are virtually equivalent, with a slight (but not always statistically sigificant) superiority of the generalized model. However, this is *not*

to be interpreted as evidence that the coupling effects are insignificant (see above).

- The present work suggests a synthesis. One can use the conventional relative permeability coefficients to describe the macroscopic behavior of steady-state co-current two-phase flow, but one should not lose sight of the fact that significant portions of their magnitudes, expressed by the coupling indices $\chi_i$, are caused by coupling effects. (This simple approach does *not* apply to situations involving steep macroscopic gradients of the saturation and the capillary pressure, such as displacements fronts, etc.)
- The magnitudes of the coupling effects, and the flow mechanisms that produce them, are of fundamental importance for the development of a satisfactory (self-consistent) quantitative model or computer-aided simulator.

## Acknowledgements

This work was supported by Shell Research B.V., Koninklijke/Shell, Exploratie en Produktie Laboratorium (KSEPL), and the Institute of Chemical Engineering and High Temperature Chemical Processes.

## References

1. Amaefule, J. O., and Handy, L. L.: 1982, The effects of interfacial tensions on relative oil/water permeabilities of consolidated porous media, *Soc. Petrol. Eng. J.* June, 371–381.
2. Archer, J. S., and Wong, S. W.: 1973, Use of a reservoir simulator to interpret laboratory waterflood data, *Soc. Petrol. Eng. J.* Dec., 343–347.
3. Auriault, J. -L.: 1987, Nonsaturated deformable porous media: Quasastatics, *Transport in Porous Media* **2**, 45–64.
4. Auriault, J.-L., Lebaigue, O., and Bonnet, G.: 1989, Dynamics of two immiscible fluids flowing through deformable porous media, *Transport in Porous Media* **4**, 105–128.
5. Avraam, D. G., Kolonis, G. B., Roumeliotis, T. C., Constantinides, G. N., and Payatakes, A. C.: 1994, Steady-state two-phase flow through planar and non-planar model porous media *Transport in Porous Media* **16**, 75–101.
6. Avraam, D. G., and Payatakes, A. C.: 1995, Flow regimes and relative permeabilities during steady-state two-phase flow in porous media, *J. Fluid Mech.* **293**, 181–206.
7. Bard, Y.: 1974, *Non-Linear Parameter Estimation*, Academic Press, New York.
8. Batycky, J. P., McCaffery, F. G., Hodgins, P. K., and Fisher, D. B.: 1981, Interpreting relative permeability and wettability from unsteady-state displacement measurements, *Soc. Petrol. Eng.* June, 296–308.
9. Bentsen, R. G.: 1974, Conditions under which the capillary term may be neglected, *J. Canad. Petrol. Technol.*, Oct.–Dec., 25–30.
10. Bentsen, R. G., and Manai, A. A.: 1993, On the use of conventional cocurrent and countercurrent effective permeabilities to estimate the four generalized permeability coefficients which arise in coupled, two-phase flow, *Transport in Porous Media* **11**, 243–262.
11. Bourbiaux, B. J., and Kalaydjian, F.: 1988, Experimental study of cocurrent and countercurrent flows in natural porous media, Paper SPE 18283, *63rd Ann. Tech. Conf. and Exhibition of SPE*, Houston.
12. Bourbiaux, B. J., and Kalaydjian, F.: 1990, Experimental study of cocurrent and countercurrent flows in natural porous media, *SPERE* **5**, 361–368.
13. Buckley, S. E., and Leverett, M. C.: 1942, Mechanism of fluid displacement in sands, *Trans. AIME* **146**, 107–116.
14. Chatzis, J. D., Morrow, N. R., and Lim, H. T.: 1983, Magnitude and detailed structure of residual oil saturation, *Soc. Petrol. Eng. J.* **23**, 311–326.

15. Chen, J. D.: 1986, Some mechanisms of immiscible fluid displacement in small networks, *J. Coll. Int. Sci.* **110**, 488–503.
16. Constantinides, G. N., and Payatakes, A. C.: 1991, A theoretical model of collision and coalescence, *J. Coll. Int. Sci.* **141**(2), 486–504.
17. De Gennes, P. G.: 1983, Theory of slow biphasic flows in porous media, *Phys. Chem. Hydrodyn.* **4**, 175–185.
18. De la Cruz, V., and Spanos, T. J. T.: 1983, Mobilization of oil ganglia, *AIChE J.* **29**, 854–858.
19. Ehrlich, R.: 1993, Viscous coupling in two-phase flow in porous media and its effect on relative permeabilities, *Transport in Porous Media* **11**, 201–218.
20. Fulcher, R. A., Ertekin, T., and Stahl, C. D.: 1985, Effect of capillary number and its constituents on two-phase relative permeability measurements, *J. Petrol. Technol.*, Feb., 249–260.
21. Goode, P. A., and Ramakrishnan, T. S.: 1993, Momentum transfer across fluid-fluid interfaces in porous media: a network model, *AIChE J.* **39**, 1124–1134.
22. Heavyside, J., Black, C. J. J., and Berry, J. F.: 1983, Fundamentals of relative permeability: Experimental and theoretical considerations, paper SPE 12173, *58th Ann. Tech. Conf. Exhib.*, San Francisco, CA, October 5–8.
23. Honarpoor, M., and Mahmood, S. M.: 1988, Relative-permeability measurements: An overview, *J. Petrol. Technol.* Aug., 963–966.
24. Ioannidis, M. A., Chatzis, I., and Payatakes, A. C.: 1991, A mercury porosimeter for investigating capillary phenomena and microdisplacement mechanisms in capillary networks, *J. Coll. Int. Sci.* **143**, 22–36.
25. Jerault, G. R., and Salter, S. J.: 1990, The effect of pure structure on hysteresis in relaive permeability and capillary pressure: Pore-level modeling, *Transport in Porous Media* **5**, 103–151.
26. Johnson, E. F., Bossler, D. R., and Naumann, V. O.: 1959, Calculation of relative permeability from displacement experiments, *Trans. AIME* **216**, 370–372.
27. Jones, S. C., and Roszelle, W. O.: 1978, Graphical techniques for determining relative permeability from displacement experiments, *J. Petrol. Technol.* May, 807–817.
28. Kalaydjian, F.: 1987, A macroscopic description of multiphase flow in porous media involving evolution of fluid/fluid interface, *Transport in Porous Media* **2**, 537–552.
29. Kalaydjian, F., and Legait, B.: 1987a, Ecoulement lent a contre-courant de deux fluides non miscibles dans un capillaire présentant un rétrecissement, *C. R. Acad. Sci. Paris, Ser. II.* **304**, 869–872.
30. Kalaydjian, F., and Legait, B.: 1987b, Perméabilités relatives couplées dans des écoulement en capillaire et en milieu poreux, *C. R. Acad. Sci. Paris, Ser. II* **304**, 1035–1038.
31. Kalaydjian, F., Bourbiaux, B., and Guerillot, D.: 1989, Viscous coupling between fluid phases for two-phase flow in porous media: theory versus experiment, *Eur. Symp. on Improved Oil Recovery*, Budapest, Hungary.
32. Kalaydjian, F.: 1990, Origin and quantification of coupling between relative permeabilities for two-phase flows in porous media, *Transport in Porous Media* **5**, 215–229.
33. Kerig. P. D., and Watson, A. T.: 1986, Relative-permeability estimation from displacement experiments: An error analysis, *Soc. Petrol. Eng.* March, 175–182.
34. Lefebvre Du Prey, E. J.: 1973, Factors affecting liquid-liquid relative permeabilities of a consolidated porous medium, *Soc. Petrol. Eng. J.* Feb., 39–47.
35. Lelievre, R. F.: 1966, Etude d'écoulements diphasiques permanent a contre-courants en milieux–Comparison avec les écoulements de meme sens. Ph.D. Thesis University of Toulouse, France.
36. Lenormand, R., Zarcone, C., and Sarr, A.: 1983, Mechanisms of the displacement of one fluid by another in a network of capillary ducts, *J. Fluid Mech.* **135**, 337–355.
37. Leverett, M. C.: 1941, Capillary behavior in porous solids, *Trans AIME* **142**, 159–169.
38. Marle, C. M.: 1982, On macroscopic equations governing multiphase flow with diffusion and chemical reactions in porous media, *Int. J. Eng. Sci.* **20**, 643–662.
39. McCaffery, F. G., and Bennion, D. W.: 1974, The effect of wettability on two-phase relative permeabilities, *J. Canad. Petrol. Technol.* Oct.–Dec., 42–53.
40. Morrow, N. R., and McCaffery, F. G.: 1978, in G. F. Padday (ed), *Wetting, Spreading, and Adhesion*, Academic Press, New York.

41. Naar, J., Wygal, G. R., and Henderson, J. H.: 1962, Imbibition relative permeability in unconsolidated porous media, *Soc. Petr. Eng. J.* **2**, 13–23.
42. Odeh, A. S.: 1959, Effect of viscosity ratio on relative permeability, *J. Petrol. Technol.* **11**, 346–354.
43. Owens, W. W., and Archer, D. L.: 1971, The effect of rock wettability on oil–water relative permeability relationships, *J. Petrol. Technol.* July, 873–878.
44. Raats, P. A. C., and Klute, A.: 1968, Transport in soils: The balance of momentum, *Soil Sci. Soc. Am. J.* **32**, 452–166.
45. Rapoport, L. A., and Leas, W. J.: 1953, Properties of linear waterfloods, *Trans. AIME*, **198**, 139–148.
46. Richards, L. A.: 1931, Capillary conduction of liquids through porous mediums, *Physics*, **1**, 318–333.
47. Rose, W.: 1972, *Fundamentals of Transport Phenomena in Porous Media*, IAHR, Elsevier, New York.
48. Rose, W.: 1988, Measuring transport coefficients necessary for the description of coupled two-phase flow of immiscible fluids in porous media, *Transport in Porous Media* **3**, 163–171.
49. Rose, W.: 1989, Data interpretation problems to be expected in the study of coupled two-phase flow of immiscible fluid flows in porous media, *Transport in Porous Media* **4**, 185–198.
50. Rose, W.: 1991, Richards' assumptions and Hassler's presumptions, *Transport in Porous Media* **6**, 91–99.
51. Sanchez-Palencia, E.: 1974, Compartiment local et macroscopique d'un type de milieux physiques et heterogenes, *Int. J. Engn. Sci.* **12**, 331–351.
52. Sandberg, C. R., Gournay, L. S., and Sippel, R. F.: 1958, The effect of fluid-flow rate and viscosity on laboratory determinations of oil-water relative permeabilities, *Trans. AIME* **213**, 36–43.
53. Sigmund, P. M., and McCaffery, F. G.: 1979, An improved unsteady-state procedure for determining the relative permeability characteristics of heterogeneous porous media, *Soc. Petrol. Eng. J.* Feb., 15–28.
54. Spanos, T. J. T., de la Cruz, V., Hube, J., and Sharma, R. C.: 1986, An analysis of Buckley–Leverett theory, *J. Can. Petr. Tech.* **25**(1), 71–75.
55. Taber, J. J.: 1958, The injection of detergent slugs in water floods, *Trans. AIME* **213**, 186–192.
56. Tao, T. M., and Watson, A. T.: 1984, Accuracy of JBN estimates of relative permeability, Part 1, Error analysis, *Soc. Petrol. Eng.* Apr., 215–224.
57. Vizika, O., and Payatakes, A. C.: 1989, Parametric experimental study of forced imbibition in porous media, *Phys. Chem. Hydrodyn.* **11**, 187–204.
58. Wardlaw, N. C.: 1982, The effects of geometry, wettability, viscosity and interfacial tension on trapping in single pore-throat pairs, *J. Canad. Petrol. Technol.* **21**, 21–27.
59. Watson, A. T., Richmond, P. C., Kerig, P. D., and Tao, T. M.: 1988, A regression-based method for estimating relative permeabilities from displacement experiments, *SPERE*, Aug., 953–958.
60. Welge, H. L.: 1952, A simplified method for computing oil recovery by gas or water drive, *Trans. AIME*, **195**, 91–98.
61. Whitaker. S.: 1986, Flow in porous media, II. The governing equations for immiscible two-phase flow, *Transport in Porous Media*, **1**, 105–125.
62. Wright, R. J., and Dawe, R. A.: 1980, An examination of the multiphase Darcy model of fluid displacement in porous media, *Rev. Inst. Franç. Petrole* Nov.–Dec. **XXXV**(6), 1011–1024.
63. Yadav, G. D., Dullien, F. A. L., Chatzis, I., and McDonald, I. F.: 1987, Microscopic distribution of wetting and nonwetting phases in sandstones during immiscible displacement, *SPERE* **2**, 137–147.
64. Yortsos, Y. C., and Fokas, A. S.: 1983, An analytical solution for linear waterflood including the effects of capillary pressure, *Soc Petrol. Eng. J.* **23**, 115–124.
65. Yuster, S. T.: 1951, Theoretical considerations of multiphase flow in idealized capillary systems, *World Petroleum Cong. Proc., Section II. Drilling and Production*, The Hague.